Sequence of V1, V2, and V3 regions of SHIV-MK38

SHIV-MK38 viral stock was used as a template for RT-PCR to amplify the V1 to V3 regions of the *env* gene. The forward primer 5′ GTGTAAAATTAACCCCACTCTGTG 3′ and reverse primer 5′ TGGGAGGGGCATACATTGCTTTTCC 3′ were used for RT-PCR. The amplified DNA fragment was cloned into the pCR2.1 vector using a TA Cloning Kit (Invitrogen, Carlsbad, CA), and 14 clones were sequenced.

Acknowledgments

We thank Dr. Julie Strizki, Schering Plough Research Institute, for providing AD101. This work was supported, in part, by Research on Human Immunodeficiency Virus/AIDS in Health and Labor Sciences research grants from the Ministry of Health, Labor and Welfare, Japan, a grant-in-aid for scientific research from the Ministry of Education and Science, Japan, a research grant for health sciences focusing on drug innovation for AIDS from the Japan Health Sciences Foundation, and a grant from the Program for the Promotion of Fundamental Studies in Health Sciences of the National Institute of Biomedical Innovation (NIBIO) of Japan.

Appendix A. Supplementary data

Supplementary data associated with this article can be found, in the online version, at doi:10.1016/j.virol.2010.01.008.

References

Baba, T.W., Liska, V., Hofmann-Lehmann, R., Vlasak, J., Xu, W., Ayehunie, S., Cavacini, L.A., Posner, M.R., Katinger, H., Stiegler, G., Bernacky, B.J., Rizvi, T.A., Schmidt, R., Hill, L.R., Keeling, M.E., Lu, Y., Wright, J.E., Chou, T.C., Ruprecht, R.M., 2000. Human neutralizing monoclonal antibodies of the IgG1 subtype protect against mucosal simian–human immunodeficiency virus infection. Nat. Med. 6 (2), 200–206.

Cardozo, T., Kimura, T., Philpott, S., Weiser, B., Burger, H., Zolla-Pazner, S., 2007. Structural basis for coreceptor selectivity by the HIV type 1 V3 loop. AIDS Res. Hum. Retroviruses 23 (3), 415–426.

Cho, M.W., Lee, M.K., Carney, M.C., Berson, J.F., Doms, R.W., Martin, M.A., 1998. Identification of determinants on a dualtropic human immunodeficiency virus type 1 envelope glycoprotein that confer usage of CXCR4. J. Virol. 72 (3), 2509–2515.

Clapham, P.R., McKnight, A., 2002. Cell surface receptors, virus entry and tropism of primate lentiviruses. J. Gen. Virol. 83 (Pt 8), 1809–1829.

de Mendoza, C., Van Baelen, K., Poveda, E., Rondelez, E., Zahonero, N., Stuyver, L., Garrido, C., Villacian, J., Soriano, V., Spanish HIV Seroconverter Study Group, 2008. Performance of a population-based HIV-1 tropism phenotypic assay and correlation with V3 genotypic prediction tools in recent HIV-1 seroconverters. J. Acquir. Immune. Defic. Syndr. 48 (3), 241–244.

Dey, B., Svehla, K., Xu, L., Wycuff, D., Zhou, T., Voss, G., Phogat, A., Chakrabarti, B.K., Li, Y., Shaw, G., Kwong, P.D., Nabel, G.J., Mascola, J.R., Wyatt, R.T., 2009. Structure-based stabilization of HIV-1 gp120 enhances humoral immune responses to the induced co-receptor binding site. PLoS Pathog. 5 (5), e1000445.

Donzella, G.A., Schols, D., Lin, S.W., Este, J.A., Nagashima, K.A., Maddon, P.J., Allaway, G.P., Sakmar, T.P., Henson, G., De Clercq, E., Moore, J.P., 1998. AMD3100, a small molecule inhibitor of HIV-1 entry via the CXCR4 co-receptor. Nat. Med. 4, 72–77.

Dorr, P., Westby, M., Dobbs, S., Griffin, P., Irvine, B., Macartney, M., Mori, J., Rickett, G., Smith-Burchnell, C., Napier, C., Webster, R., Armour, D., Price, D., Stammen, B., Wood, A., Perros, M., 2005. Maraviroc (UK-427,857), a potent, orally bioavailable, and selective small-molecule inhibitor of chemokine receptor CCR5 with broad-spectrum anti-human immunodeficiency virus type 1 activity. Antimicrob. Agents. Chemother. 49 (11), 4721–4732.

Fätkenheuer, G., Pozniak, A.L., Johnson, M.A., Plettenberg, A., Staszewski, S., Hoepelman, A.I., Saag, M.S., Goebel, F.D., Rockstroh, J.K., Dezube, B.J., Jenkins, T.M., Medhurst, C., Sullivan, J.F., Ridgway, C., Abel, S., James, I.T., Youle, M., van der Ryst, E., 2005. Efficacy of short-term monotherapy with maraviroc, a new CCR5 antagonist, in patients infected with HIV-1. Nat. Med. 11 (11), 1170–1172 Epub 2005 Oct 5.

Feinberg, M.B., Moore, J.P., 2002. AIDS vaccine models: challenging challenge viruses. Nat. Med 8 (3), 207–210.

Fukazawa, Y., Miyake, A., Ibuki, K., Inaba, K., Saito, N., Motohara, M., Horiuchi, R., Himeno, A., Matsuda, K., Matsuyama, M., Takahashi, H., Hayami, M., Igarashi, T., Miura, T., 2008. Small intestine CD4+ T cells are profoundly depleted during acute simian–human immunodeficiency virus infection, regardless of viral pathogenicity. J. Virol. 82 (12), 6039–6044.

Harouse, J.M., Gettie, A., Tan, R.C., Blanchard, J., Cheng-Mayer, C., 1999. Distinct pathogenic sequela in rhesus macaques infected with CCR5 or CXCR4 utilizing SHIVs. Science 30 (284(5415)), 816–819.

Hessell, A.J., Rakasz, E.G., Poignard, P., Hangartner, L., Landucci, G., Forthal, D.N., Koff, W. C., Watkins, D.I., Burton, D.R., 2009. Broadly neutralizing human anti-HIV antibody 2G12 is effective in protection against mucosal SHIV challenge even at low serum neutralizing titers. PLoS Pathog. 5 (5), e1000433.

Ho, S.H., Shek, L., Gettie, A., Blanchard, J., Cheng-Mayer, C., 2005. V3 loop-determined coreceptor preference dictates the dynamics of CD4+-T-cell loss in simian–human immunodeficiency virus-infected macaques. J. Virol. 79 (19), 12296–12303.

Ho, S.H., Tasca, S., Shek, L., Li, A., Gettie, A., Blanchard, J., Boden, D., Cheng-Mayer, C., 2007. Coreceptor switch in R5-tropic simian/human immunodeficiency virus-infected macaques. J. Virol. 81 (16), 8621–8633.

Humbert, M., Rasmussen, R.A., Song, R., Ong, H., Sharma, P., Chenine, A.L., Kramer, V.G., Siddappa, N.B., Xu, W., Else, J.G., Novembre, F.J., Strobert, E., O'Neil, S.P., Ruprecht, R.M., 2008. SHIV-1157i and passaged progeny viruses encoding R5 HIV-1 clade C env cause AIDS in rhesus monkeys. Retrovirology 17 (5), 94.

Igarashi, T., Endo, Y., Englund, G., Sadjadpour, R., Matano, T., Buckler, C., Buckler-White, A., Plishka, R., Theodore, T., Shibata, R., Martin, M., 1999. Emergence of a highly pathogenic simian/human immunodeficiency virus in a rhesus macaque treated with anti-CD8 mAb during a primary infection with a nonpathogenic virus. Proc. Natl. Acad. Sci. U. S. A. 96 (24), 14049–14054.

Igarashi, T., Donau, O.K., Imamichi, H., Dumaurier, M.J., Sadjadpour, R., Plishka, R.J., Buckler-White, A., Buckler, C., Suffredini, A.F., Lane, H.C., Moore, J.P., Martin, M.A., 2003. Macrophage-tropic simian/human immunodeficiency virus chimeras use CXCR4, not CCR5, for infections of rhesus macaque peripheral blood mononuclear cells and alveolar macrophages. J. Virol. 77 (24), 13042–13052.

Kozyrev, I.L., Miura, T., Takemura, T., Kuwata, T., Ui, M., Ibuki, K., Iida, T., Hayami, M., 2002. Co-expression of interleukin-5 influences replication of simian/human immunodeficiency viruses in vivo. J. Gen. Virol. 83, 1183–1188.

Jensen, M.A., Li, F.S., van 't Wout, A.B., Nickle, D.C., Shriner, D., He, H.X., McLaughlin, S., Shankarappa, R., Margolick, J.B., Mullins, J.I., 2003. Improved coreceptor usage prediction and genotypic monitoring of R5-to-X4 transition by motif analysis of human immunodeficiency virus type 1 env V3 loop sequences. J. Virol. 77 (24), 13376–13388.

Kestler III, H.W., Ringler, D.J., Mori, K., Panicali, D.L., Sehgal, P.K., Daniel, M.D., Desrosiers, R.C., 1991. Importance of the nef gene for maintenance of high virus loads and for development of AIDS. Cell 65 (4), 651–662.

Laird, M.E., Igarashi, T., Martin, M.A., Desrosiers, R.C., 2008. Importance of the V1/V2 loop region of simian–human immunodeficiency virus envelope glycoprotein gp120 in determining the strain specificity of the neutralizing antibody response. J. Virol. 82 (22), 11054–11065.

Li, M., Gao, F., Mascola, J.R., Stamatatos, L., Polonis, V.R., Koutsoukos, M., Voss, G., Goepfert, P., Gilbert, P., Greene, K.M., Bilska, M., Kothe, D.L., Salazar-Gonzalez, J.F., Wei, X., Decker, J.M., Hahn, B.H., Montefiori, D.C., 2005. Human immunodeficiency virus type 1 env clones from acute and early subtype B infections for standardized assessments of vaccine-elicited neutralizing antibodies. J. Virol. 79 (16), 10108–10125.

Luciw, P.A., Pratt-Lowe, E., Shaw, K.E., Levy, J.A., Cheng-Mayer, C., 1995. Persistent infection of rhesus macaques with T-cell-line-tropic and macrophage-tropic clones of simian/human immunodeficiency viruses (SHIV). Proc. Natl. Acad. Sci. U. S. A. 92 (16), 7490–7494.

Marcon, L., Choe, H., Martin, K.A., Farzan, M., Ponath, P.D., Wu, L., Newman, W., Gerard, N., Gerard, C., Sodroski, J., 1997. Utilization of C-C chemokine receptor 5 by the envelope glycoproteins of a pathogenic simian immunodeficiency virus, SIV-mac239. J. Virol. 71 (3), 2522–2527.

Margolis, L., Shattock, R., 2006. Selective transmission of CCR5-utilizing HIV-1: the 'gatekeeper' problem resolved? Nat. Rev. Microbiol. 4 (4), 312–317.

Mascola, J.R., Stiegler, G., VanCott, T.C., Katinger, H., Carpenter, C.B., Hanson, C.E., Beary, H., Hayes, D., Frankel, S.S., Birx, D.L., Lewis, M.G., 2000. Protection of macaques against vaginal transmission of a pathogenic HIV-1/SIV chimeric virus by passive infusion of neutralizing antibodies. Nat. Med. 6 (2), 207–210.

Mefford, M.E., Gorry, P.R., Kunstman, K., Wolinsky, S.M., Gabuzda, D., 2008. Bioinformatic prediction programs underestimate the frequency of CXCR4 usage by R5X4 HIV type 1 in brain and other tissues. AIDS Res. Hum. Retroviruses 24 (9), 1215–1220.

Miyake, A., Ibuki, K., Enose, Y., Suzuki, H., Horiuchi, R., Motohara, M., Saito, N., Nakasone, T., Honda, M., Watanabe, T., Miura, T., Hayami, M., 2006. Rapid dissemination of a pathogenic simian/human immunodeficiency virus to systemic organs and active replication in lymphoid tissues following intrarectal infection. J. Gen. Virol. 87, 1311–1320.

Nishimura, Y., Igarashi, T., Donau, O.K., Buckler-White, A., Buckler, C., Lafont, B.A., Goeken, R.M., Goldstein, S., Hirsch, V.M., Martin, M.A., 2004. Highly pathogenic SHIVs and SIVs target different CD4+ T cell subsets in rhesus monkeys, explaining their divergent clinical courses. Proc. Natl. Acad. Sci. U. S. A. 101 (33), 12324–12329.

O'Doherty, U., Swiggard, W.J., Malim, M.H., 2000. Human immunodeficiency virus type 1 spinoculation enhances infection through virus binding. J. Virol. 74, 10074–10080.

Pastore, C., Ramos, A., Mosier, D.E., 2000. Intrinsic obstacles to human immunodeficiency virus type 1 coreceptor switching. J. Virol. 74 (15), 6769–6776.

Pitcher, C.J., Hagen, S.I., Walker, J.M., Lum, R., Mitchell, B.L., Maino, V.C., Axthelm, M.K., Picker, L.J., 2002. Development and homeostasis of T cell memory in rhesus macaque. J. Immunol. 168 (1), 29–43.

Reimann, K.A., Li, J.T., Veazey, R., Halloran, M., Park, I.W., Karlsson, G.B., Sodroski, J., Letvin, N.L., 1996. A chimeric simian/human immunodeficiency virus expressing a primary patient human immunodeficiency virus type 1 isolate env causes an AIDS-like disease after in vivo passage in rhesus monkeys. J. Virol. 70 (10), 6922–6928.

Sadjadpour, R., Theodore, T.S., Igarashi, T., Donau, O.K., Plishka, R.J., Buckler-White, A., Martin, M.A., 2004. Induction of disease by a molecularly cloned highly pathogenic simian immunodeficiency virus/human immunodeficiency virus chimera is multigenic. J. Virol. 78, 5513–5519.

Sagar, M., Wu, X., Lee, S., Overbaugh, J., 2006. Human immunodeficiency virus type 1 V1-V2 envelope loop sequences expand and add glycosylation sites over the course of infection, and these modifications affect antibody neutralization sensitivity. J. Virol. 80 (19), 9586–9598.

Shibata, R., Kawamura, M., Sakai, H., Hayami, M., Ishimoto, A., Adachi, A., 1991. Generation of a chimeric human and simian immunodeficiency virus infectious to monkey peripheral blood mononuclear cells. J. Virol. 65 (7), 3514–3520.

Shimizu, Y., Okoba, M., Yamazaki, N., Goto, Y., Miura, T., Hayami, M., Hoshino, H., Haga, T., 2006. Construction and in vitro characterization of a chimeric simian and human immunodeficiency virus with the RANTES gene. Microbes. Infect. 8 (1), 105–113.

Shinohara, K., Sakai, K., Ando, S., Ami, Y., Yoshino, N., Takahashi, E., Someya, K., Suzaki, Y., Nakasone, T., Sasaki, Y., Kaizu, M., Lu, Y., Honda, M., 1999. A highly pathogenic simian/human immunodeficiency virus with genetic changes in cynomolgus monkey. J. Gen. Virol. 80, 1231–1240.

Shiver, J.W., Fu, T.M., Chen, L., Casimiro, D.R., Davies, M.E., Evans, R.K., Zhang, Z.Q., Simon, A.J., Trigona, W.L., Dubey, S.A., Huang, L., Harris, V.A., Long, R.S., Liang, X., Handt, L., Schleif, W.A., Zhu, L., Freed, D.C., Persaud, N.V., Guan, L., Punt, K.S., Tang, A., Chen, M., Wilson, K.A., Collins, K.B., Heidecker, G.J., Fernandez, V.R., Perry, H.C., Joyce, J.G., Grimm, K.M., Cook, J.C., Keller, P.M., Kresock, D.S., Mach, H., Troutman, R.D., Isopi, L.A., Williams, D.M., Xu, Z., Bohannon, K.E., Volkin, D.B., Montefiori, D.C., Miura, A., Krivulka, G.R., Lifton, M.A., Kuroda, M.J., Schmitz, J.E., Letvin, N.L., Caulfield, M.J., Bett, A.J., Youil, R., Kaslow, D.C., Emini, E.A., 2002. Replication-incompetent adenoviral vaccine vector elicits effective anti-immunodeficiency-virus immunity. Nature 415 (6869), 331–335.

Sing, T., Low, A.J., Beerenwinkel, N., Sander, O., Cheung, P.K., Domingues, F.S., Büch, J., Däumer, M., Kaiser, R., Lengauer, T., Harrigan, P.R., 2007. Predicting HIV coreceptor usage on the basis of genetic and clinical covariates. Antivir. Ther. 12 (7), 1097–1106.

Tan, R.C., Harouse, J.M., Gettie, A., Cheng-Mayer, C., 1999. In vivo adaptation of SHIV (SF162): chimeric virus expressing a NSI, CCR5-specific envelope protein. J. Med. Primatol. 28 (4-5), 164–168.

Trkola, A., Kuhmann, S.E., Strizki, J.M., Maxwell, E., Ketas, T., Morgan, T., Pugach, P., Xu, S., Wojcik, L., Tagat, J., Palani, A., Shapiro, S., Clader, J.W., McCombie, S., Reyes, G.R., Baroudy, B.M., Moore, J.P., 2002. HIV-1 escape from a small molecule, CCR5-specific entry inhibitor does not involve CXCR4 use. Proc. Natl. Acad. Sci. U.S.A. 99, 395–400.

Veazey, R.S., DeMaria, M., Chalifoux, L.V., Shvetz, D.E., Pauley, D.R., Knight, H.L., Rosenzweig, M., Johnson, R.P., Desrosiers, R.C., Lackner, A.A., 1998. Gastrointestinal tract as a major site of CD4+ T cell depletion and viral replication in SIV infection. Science 280 (5362), 427–431.

Wei, X., Decker, J.M., Wang, S., Hui, H., Kappes, J.C., Wu, X., Salazar-Gonzalez, J.F., Salazar, M.G., Kilby, J.M., Saag, M.S., Komarova, N.L., Nowak, M.A., Hahn, B.H., Kwong, P.D., Shaw, G.M., 2003. Antibody neutralization and escape by HIV-1. Nature 422 (6929), 307–312.

Willey, R.L., Smith, D.H., Lasky, L.A., Theodore, T.S., Earl, P.L., Moss, B., Capon, D.J., Martin, M.A., 1988. In vitro mutagenesis identifies a region within the envelope gene of the human immunodeficiency virus that is critical for infectivity. J. Virol. 62 (1), 139–147.

Yamaguchi-Kabata, Y., Yamashita, M., Ohkura, S., Hayami, M., Miura, T., 2004. Linkage of amino acid variation and evolution of human immunodeficiency virus type 1 gp120 envelope glycoprotein (subtype B) with usage of the second receptor. J. Mol. Evol. 58 (3), 333–340.

Zhang, Y., Lou, B., Lal, R.B., Gettie, A., Marx, P.A., Moore, J.P., 2000. Use of inhibitors to evaluate coreceptor usage by simian and simian/human immunodeficiency viruses and human immunodeficiency virus type 2 in primary cells. J. Virol. 74 (15), 6893–6910.

Web references

Web PSSM, Mullins Lab, University of Washington http://indra.mullins.microbiol.washington.edu/webpssm/

Geno2pheno [coreceptor], Max-Planck-Institut Informatik. http://coreceptor.bioinf.mpi-inf.mpg.de

Journal of General Virology (2010), 91, 773–781 DOI 10.1099/vir.0.017368-0

Small intestine $CD4^+$ cell reduction and enteropathy in simian/human immunodeficiency virus KS661-infected rhesus macaques in the presence of low viral load

Katsuhisa Inaba,[1] Yoshinori Fukazawa,[1] Kenta Matsuda,[1] Ai Himeno,[1] Megumi Matsuyama,[1] Kentaro Ibuki,[1] Yoshiharu Miura,[2] Yoshio Koyanagi,[2] Atsushi Nakajima,[3] Richard S. Blumberg,[4] Hidemi Takahashi,[5] Masanori Hayami,[1] Tatsuhiko Igarashi[1] and Tomoyuki Miura[1]

Correspondence
Tomoyuki Miura
tmiura@virus.kyoto-u.ac.jp

[1]Laboratory of Primate Model, Experimental Research Center for Infectious Diseases, Institute for Virus Research, Kyoto University, 53 Shogoinkawaramachi, Sakyo-ku, Kyoto 606-8507, Japan

[2]Laboratory of Viral Pathogenesis, Institute for Virus Research, Kyoto University, 53 Shogoinkawaramachi, Sakyo-ku, Kyoto 606-8507, Japan

[3]Division of Gastroenterology, Yokohama City University Graduate School of Medicine, Yokohama, Japan

[4]Division of Gastroenterology, Brigham and Women's Hospital, Harvard Medical School, Boston, MA, USA

[5]Department of Microbiology and Immunology, Nippon Medical School, Tokyo, Japan

Human immunodeficiency virus type 1, simian immunodeficiency virus and simian/human immunodeficiency virus (SHIV) infection generally lead to death of the host accompanied by high viraemia and profound $CD4^+$ T-cell depletion. SHIV clone KS661-infected rhesus macaques with a high viral load set point (HVL) ultimately experience diarrhoea and wasting at 6–12 months after infection. In contrast, infected macaques with a low viral load set point (LVL) usually live asymptomatically throughout the observation period, and are therefore referred to as asymptomatic LVL (Asym LVL) macaques. Interestingly, some LVL macaques exhibit diarrhoea and wasting similar to the symptoms of HVL macaques and are termed symptomatic LVL (Sym LVL) macaques. This study tested the hypothesis that Sym LVL macaques have the same degree of intestinal abnormalities as HVL macaques. The proviral DNA loads in lymphoid tissue and the intestines of Sym LVL and Asym LVL macaques were comparable and all infected monkeys showed villous atrophy. Notably, the $CD4^+$ cell frequencies of lymphoid tissues and intestines in Sym LVL macaques were remarkably lower than those in Asym LVL and uninfected macaques. Furthermore, Sym LVL and HVL macaques exhibited an increased number of activated macrophages. In conclusion, intestinal disorders including $CD4^+$ cell reduction and abnormal immune activation can be observed in SHIV-KS661-infected macaques independent of virus replication levels.

Received 5 October 2009
Accepted 3 November 2009

INTRODUCTION

The intestinal tract, which is the largest mucosal and lymphoid organ and which contains the majority of the total lymphocytes in the body, is an important port of entry for human immunodeficiency virus type 1 (HIV-1) infection in vertical and homosexual transmission (Smith *et al.*, 2003). Additionally, the intestinal tract is a central site in the interaction between HIV-1 and its host, and suffers profound pathological changes as a result of HIV-1 infection. HIV-1 infection of the intestinal tract is characterized by virus replication (Fackler *et al.*, 1998), $CD4^+$ T-cell depletion (Brenchley *et al.*, 2004), opportunistic infection and HIV enteropathy, which is an idiopathic intestinal disorder observed in infected patients with diarrhoea (Kotler, 2005). In particular, $CD4^+$ T-cell depletion, which is the immunological hallmark in the development of AIDS, preferentially takes place in the intestinal tract rather than in the peripheral blood throughout the infection (Brenchley *et al.*, 2004). This

observation is based on the following findings: (i) most naturally transmitted HIV-1 strains are chemokine receptor 5 (CCR5)-tropic; and (ii) the intestinal tract, especially the lamina propria, contains a large number of activated memory $CCR5^+$ $CD4^+$ T cells, which indicates a high susceptibility for HIV-1 infection, whereas the peripheral blood has a relatively small population of these cells (Anton *et al.*, 2000; Lapenta *et al.*, 1999). $CD4^+$ T-cell depletion from the intestinal tract by HIV-1 infection is thought to lead to progressive dysfunction of mucosal immunity, which triggers immunodeficiency (Paiardini *et al.*, 2008). In addition to $CD4^+$ T-cell depletion in the intestinal tract, HIV-1 infection causes histopathological changes in the intestine, including villous atrophy, crypt hyperplasia and acute/chronic inflammation (Batman *et al.*, 1989).

Chronic disease of the intestinal tract generally manifests as inflammation (Kahn, 1997). Diarrhoea is a major intestinal symptom caused by various stimuli to the intestinal tract such as pathogens, toxins and dysfunction of the immune system (Gibbons & Fuchs, 2007). Because HIV-1 infection weakens the host immune system, AIDS is one of the primary causes of chronic diarrhoea (Sestak, 2005). In developing countries, diarrhoea was a major symptom in advanced HIV-1 infection prior to the establishment of highly active antiretroviral therapy (HAART) (Wilcox & Saag, 2008). Dehydration and malabsorption as a result of chronic diarrhoea can lead to progressive weight loss and can contribute to morbidity and mortality in HIV-1-infected patients (Sharpstone & Gazzard, 1996). Therefore, chronic diarrhoea is one of the most important clinical signs in AIDS patients.

AIDS models using non-human primates have provided many important observations on AIDS pathogenesis. The first finding of early $CD4^+$ T-cell depletion from the intestinal tract was reported in a study using simian immunodeficiency virus (SIV)-infected macaques (Veazey *et al.*, 1998). Intestinal $CD4^+$ T cells of rhesus macaques predominantly exhibit a $CCR5^+$ activated memory phenotype, and $CD4^+$ T cells of this phenotype are selectively eliminated in SIV-infected macaques, indicating that the majority of intestinal $CD4^+$ T cells are primary targets of SIV infection (Veazey *et al.*, 2000a, b). Accordingly, detailed analysis of the intestinal tract using animal models is essential for an understanding of AIDS pathogenesis.

Simian/human immunodeficiency virus (SHIV)-KS661 is a molecular clone and a pathogenic virus in rhesus macaques. SHIV-KS661 systemically depletes $CD4^+$ T cells of rhesus macaques within 4 weeks of infection (Miyake *et al.*, 2006). Based on our observations over a number of years, intravenous infection of rhesus macaques with SHIV-KS661 consistently results in high viraemia and $CD4^+$ T-cell depletion, followed by malignant morbidity as a result of severe chronic diarrhoea and wasting after 6–18 months. Generally, the time to clinical morbidity in rhesus macaques infected with pathogenic SHIVs, such as SHIV-89.6P and SHIV-KS661, is considerably shorter than in HIV-1-infected humans, who take an average of 10 years to progress to AIDS. In addition, all subsets of $CD4^+$ T cells including memory and naïve T cells are thoroughly depleted in pathogenic SHIV-infected macaques. However, in the SHIV-KS661 macaque model, diarrhoea and wasting, which are major symptoms in advanced HIV-1 infection, can clearly be recognized and defined in association with disease progression.

Recently, we observed that, in many rhesus macaques infected intrarectally with SHIV-KS661, plasma viral RNA loads decreased gradually to undetectable levels in the chronic phase, which is quite different from the case with intravenous infection. It is well known that pathogenic SIV and SHIV infections in monkeys, like HIV-1 infections in humans, generally lead to high viraemia, profound $CD4^+$ T-cell depletion and death. Interestingly, in this study, two out of six intrarectally inoculated macaques with a low plasma viral load experienced malignant morbidity manifest as severe diarrhoea and wasting, similar to what we observed in infected macaques with high viraemia. The purpose of this study was to elucidate why macaques with a low plasma viral load experienced diarrhoea and wasting. As an explanation for this morbidity, we hypothesized that, even if the viral load set-point is suppressed, SHIV-KS661-infected macaques would have the same degree of intestinal abnormalities as infected macaques with high viraemia. To test this hypothesis, we analysed $CD4^+$ cell frequencies in lymphoid and intestinal tissues and damage to the intestinal mucosa in infected macaques with high and low viral load set points (HVL and LVL, respectively). Here, we have provided evidence for the development of intestinal disorders in SHIV-KS661-infected macaques irrespective of the plasma viral RNA load.

RESULTS

Diarrhoea and wasting in two macaques despite low viral load

All macaques inoculated intravenously with SHIV-KS661 and one out of seven macaques inoculated intrarectally with SHIV-KS661 exhibited high set points of plasma viral RNA loads, persisting at over 10^6 copies ml^{-1} until they needed to be euthanized as a result of diarrhoea and wasting (Fig. 1a). In contrast, in the remaining six macaques inoculated intrarectally with SHIV-KS661, the set points of plasma viral RNA load gradually decreased to undetectable levels (Fig. 1a). We called these macaques showing high and low set points of viral RNA load HVL and LVL macaques, respectively. During an observation period of approximately 1.4 years, two LVL macaques (MM397 and MM399) experienced severe diarrhoea and wasting and required euthanasia at approximately 22 weeks post-infection (p.i.), similar to HVL macaques, whereas the remaining four LVL macaques were asymptomatic (Fig. 1a). We termed the healthy LVL macaques asymptomatic LVL macaques (Asym LVL) and the LVL

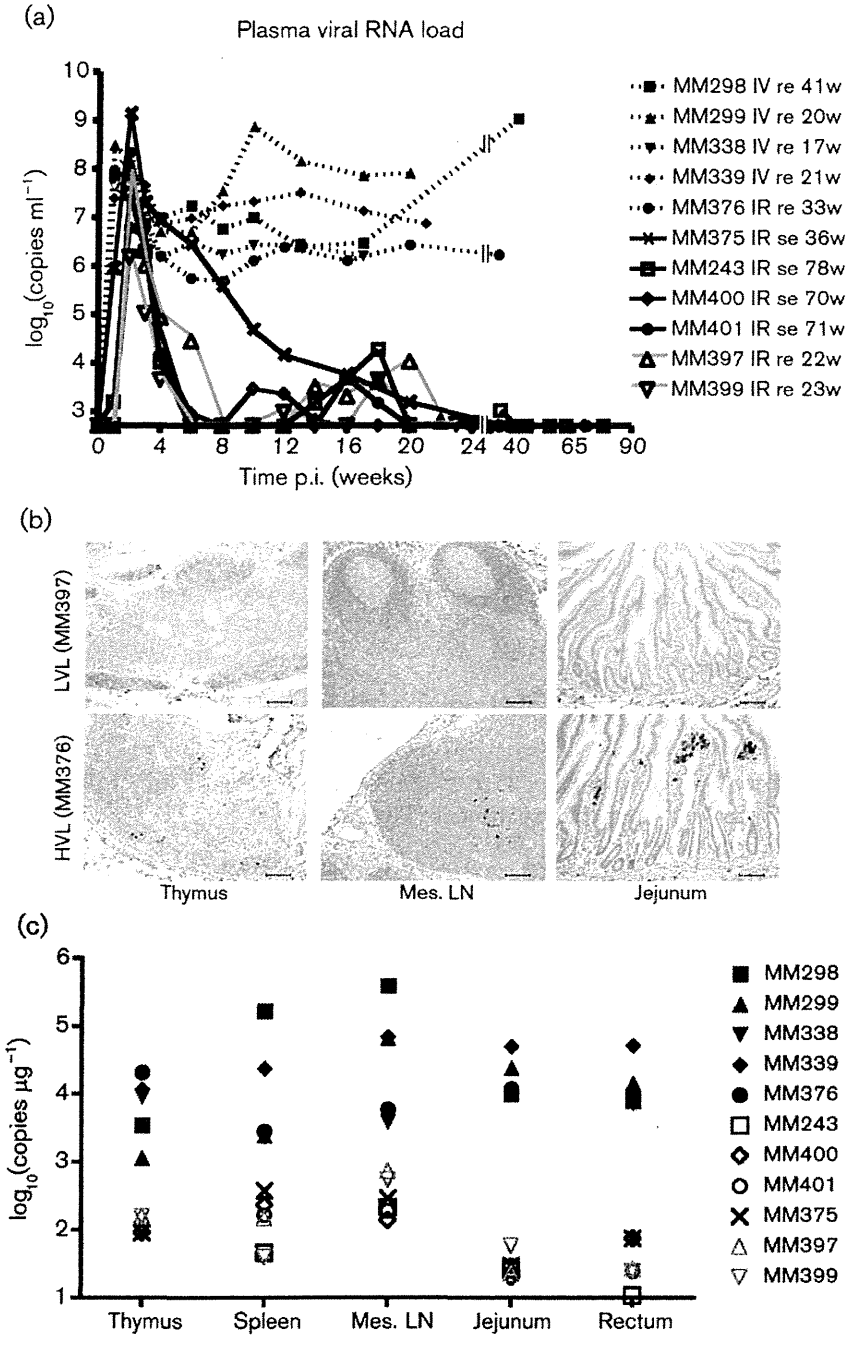

Fig. 1. Distribution of virus in various tissues of SHIV-KS661-infected rhesus macaques. (a) Time course of plasma viral RNA loads as measured by quantitative RT-PCR. The detection limit of plasma viral RNA loads was 500 copies ml^{-1}. The animal ID numbers, infection route and when and how they were euthanized are indicated on the figure. IV, Intravenous inoculation; IR, intrarectal inoculation; re, required euthanasia; se, scheduled euthanasia; w, number of weeks after infection when euthanasia was performed. (b) Immunohistochemical detection of Nef antigen in thymus, mesenteric lymph nodes (Mes. LN) and jejunum. Brown staining indicates Nef^+ cells. The upper panels show representative tissue sections from a Sym LVL macaque (MM397) and the lower panels show representative tissue sections from an HVL macaque (MM376). Bars, 100 µm. (c) Proviral DNA loads in different tissues of SHIV-KS661-infected macaques, as measured by quantitative PCR. The detection limit of proviral DNA loads was 10 copies μg^{-1}. Filled black symbols indicate HVL macaques, open black symbols indicate Asym LVL macaques and open grey symbols indicate Sym LVL macaques.

macaques with diarrhoea and wasting symptomatic LVL macaques (Sym LVL).

Antibody response against SHIV in infected macaques

The LVL macaques showed antibody responses to SHIV-KS661 at 3–4 weeks p.i. and then developed strong antibody responses that persisted up to 18 weeks p.i. (Table 1). In contrast, two of the HVL macaques (MM298 and MM299) showed no antibody response, whilst the remaining two (MM338 and MM339) showed very low antibody responses. Among the HVL macaques, only MM376 showed a strong antibody response: the titre reached 1:2048 at 6 weeks p.i., but then decreased to a much lower value. These results showed that LVL macaques succeeded in maintaining a strong antibody response, whilst HVL macaques failed to do so.

Viral levels in tissues from Sym LVL and Asym LVL macaques are not significantly different

To investigate whether the infected macaques had different viral levels in their lymphoid and intestinal tissues, we used

Table 1. Anti-HIV antibody titres in infected monkeys

– indicates a titre of <32.

Time (weeks)	Intrarectal inoculation						Intravenous inoculation			
	LVL						HVL			
	MM243	MM397	MM399	MM400	MM401	MM375	MM376	MM298	MM299	MM338	MM339
0	–	–	–	–	–	–	–	–	–	–	–
1	–	–	–	–	–	–	–	–	–	–	–
2	–	–	–	–	–	–	–	–	–	64	64
3	32	–	32	–	–	128	–	–	–	32	32
4	32	16384	32	64	32	512	512	–	–	–	–
6	8192	16384	256	64	4096	1024	2048	–	–	–	–
8	4096	16384	1024	128	1024	16384	512	–	–	–	–
10	16384	16384	2048	512	512	16384	512	–	–	–	–
12	16384	16384	256	512	4096	16384	512				
13								–	–	–	–
14	16384	16384	1024	512	2048						
16	4096	8192	1024	1024	1024	16384	64				
17								–	–	–	–
18	8192	16384	2048	8192	4096						

the Nef antigen as a marker of virus infection using immunohistochemistry and quantitative analysis of proviral DNA in lymphoid and intestinal tissues. Nef^+ cells were detected in large numbers in the tissues of HVL macaques, but were undetectable in both Sym LVL (Fig. 1b) and Asym LVL (data not shown) macaques.

In the HVL macaques, high proviral DNA loads (>1000 copies μg^{-1}) were found in all of the tissues examined (Fig. 1c). In contrast, the proviral DNA loads in the tissues of the LVL macaques were only several tens to several hundreds of copies μg^{-1} (Fig. 1c). Furthermore, Sym LVL and Asym LVL macaques exhibited comparably low proviral DNA loads in these tissues (Fig. 1c). The low viral levels in lymphoid and intestinal tissues in the LVL macaques were consistent with their set points of plasma viral RNA loads. The viral levels in lymphoid and intestinal tissues were not significantly different between Sym LVL and Asym LVL macaques.

Diarrhoea and wasting in LVL macaques correlate with $CD4^+$ cell frequency in lymphoid and intestinal tissues, but not in peripheral blood

Because $CD4^+$ T-cell depletion is the hallmark of AIDS, we first examined $CD4^+$ T-cell counts in peripheral blood. Whilst peripheral $CD4^+$ T cells were completely and irreversibly depleted in HVL macaques throughout the infection, they displayed various kinetics in LVL macaques (Fig. 2a). MM397 (Sym LVL) and MM401 (Asym LVL) had very low $CD4^+$ T-cell counts (<150 cells ml^{-1}) at all times at which they were examined after infection, whereas MM399 (Sym LVL) and MM400 (Asym LVL) maintained moderate $CD4^+$ T-cell counts (>300 cells ml^{-1}) throughout the experiment (Fig. 2a).

Naïve $CD4^+$ T cells of MM397 (Sym LVL), MM243 (Asm LVL) and MM401 (Asym LVL) were depleted as early as 4 weeks p.i., whereas those of MM399 (Sym LVL) and MM400 (Asym LVL) remained at moderate levels (Fig. 2b). The HVL macaques were not examined because their peripheral $CD4^+$ T cells were depleted.

In addition to evaluating $CD4^+$ T cells in the blood, we evaluated $CD4^+$ cells in lymphoid and intestinal tissues using CD4 staining. The HVL macaques showed severe depletion of $CD4^+$ cells in all lymphoid tissues and intestine compared with the uninfected macaques (Fig. 2c, d). Interestingly, the $CD4^+$ cell frequencies in the tissues were clearly lower in Sym LVL macaques than in uninfected macaques (Fig. 2c, d). However, the $CD4^+$ cell frequencies in the tissues of Asym LVL macaques were comparable to those in uninfected macaques. These findings indicated that the emergence of diarrhoea and wasting in LVL macaques correlated with the low $CD4^+$ cell frequency in lymphoid tissues and the intestines, but not with the counts of peripheral $CD4^+$ T-cell subsets.

Infected animals exhibit significantly shorter villi

Symptomatic animals (Sym LVL and HVL macaques) exhibited diarrhoea. To examine whether the jejunum of symptomatic animals exhibited the histopathological changes that suggest AIDS-related enteropathy, we measured villous length on haematoxylin and eosin (H&E)-stained samples of jejunum in uninfected and infected macaques. Surprisingly, villous length was significantly

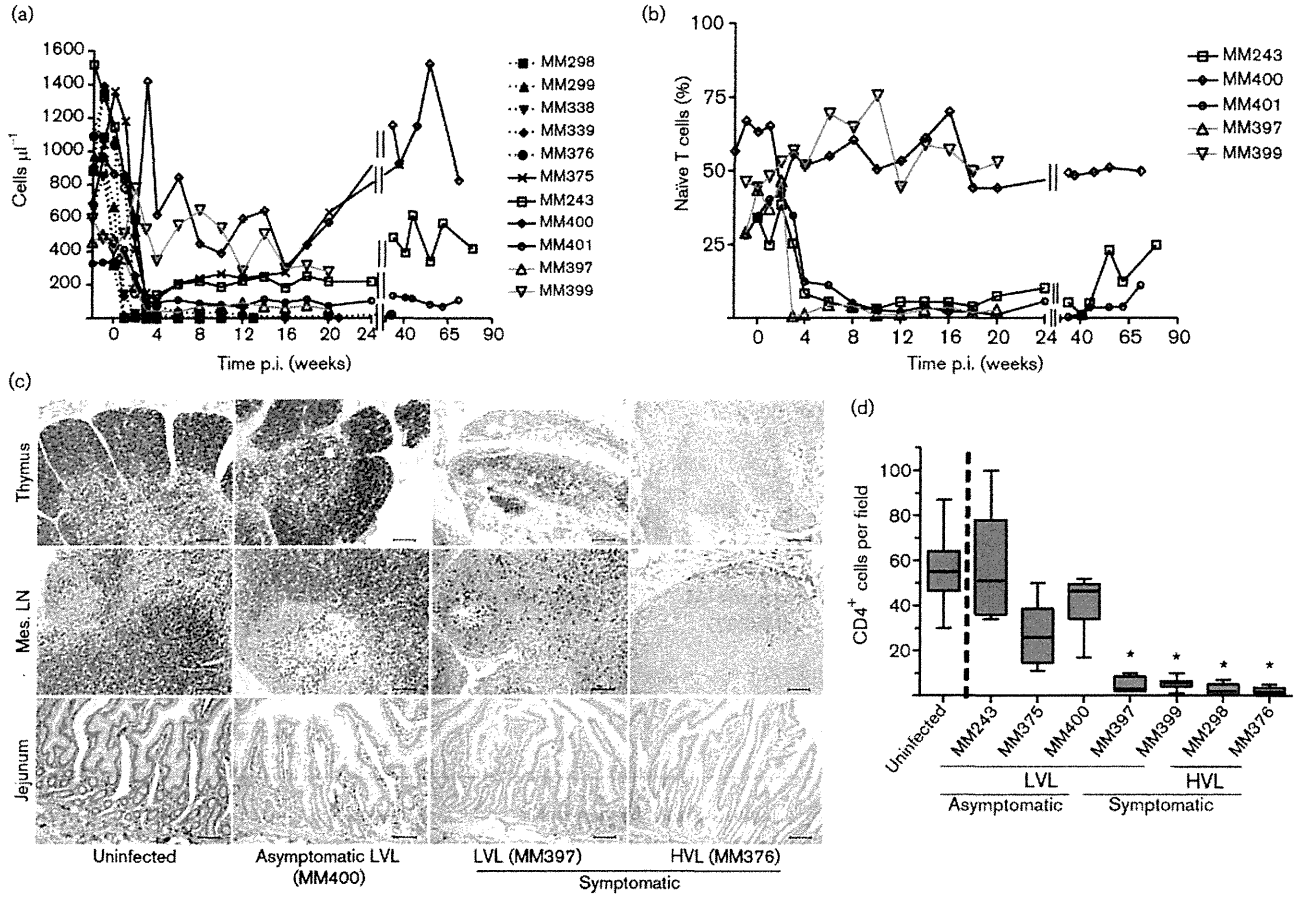

Fig. 2. Counts of circulating $CD4^+$ T-cell subsets and $CD4^+$ cell frequency in lymphoid and intestinal tissues at the time of euthanasia in SHIV-KS661-infected rhesus macaques. Counts of circulating $CD4^+$ T-cell subsets were analysed by flow cytometry and whole-blood counts. (a) Circulating $CD4^+$ T-cell counts. The ID numbers of the macaques are indicated on the figure. (b) Proportion of $CD95^+$ naïve cells in circulating $CD4^+$ T cells of LVL macaques. Solid black lines indicate Asym LVL macaques and solid grey lines indicate Sym LVL macaques. (c) $CD4^+$ cell frequencies in thymus, mesenteric lymph nodes (Mes. LN) and jejunum of representative uninfected, Asym LVL, Sym LVL and HVL macaques. Bars, 100 µm. (d) Quantification of jejunum $CD4^+$ cells in uninfected and infected macaques. The numbers of $CD4^+$ cells were enumerated in at least ten fields of the tissues at a magnification of 200×. Statistical analysis was performed using Student's *t*-test for the data from five uninfected and each infected macaque (*, $P<0.0001$). Data for MM299, MM338, MM339 and MM401 were not available.

shorter in all of the infected animals than in uninfected animals ($P<0.0001$) (Fig. 3a, b). This suggested that SHIV-infected animals develop villous atrophy, irrespective of viral load.

Increased number of activated macrophages in the jejunum of symptomatic animals

Macrophages appeared to be more abundant in H&E-stained jejunal sections in symptomatic animals. This was confirmed by CD68 staining: the frequency of $CD68^+$ macrophages in the jejunum was considerably higher in symptomatic animals than in uninfected animals, but was not significantly different between uninfected animals and Asym LVL macaques (data not shown). Furthermore, $CD68^+$ macrophages in the small intestine of Sym LVL and HVL macaques appeared to be activated because their size was increased. To examine whether the number of activated $CD68^+$ macrophages increased in the small intestine, we double stained for CD68 and Ki67 in the small intestine sections by immunohistochemistry. The frequency of $CD68^+$ $Ki67^+$ macrophages in the jejunum of all symptomatic animals examined was significantly higher than that of uninfected animals ($P<0.0001$) (Fig. 3c, d). This suggested that abnormal activation of intestinal macrophages occurred in symptomatic animals irrespective of viral load.

DISCUSSION

It is important to discuss initially why some SHIV-infected macaques had an HVL at the late stage, whilst others had

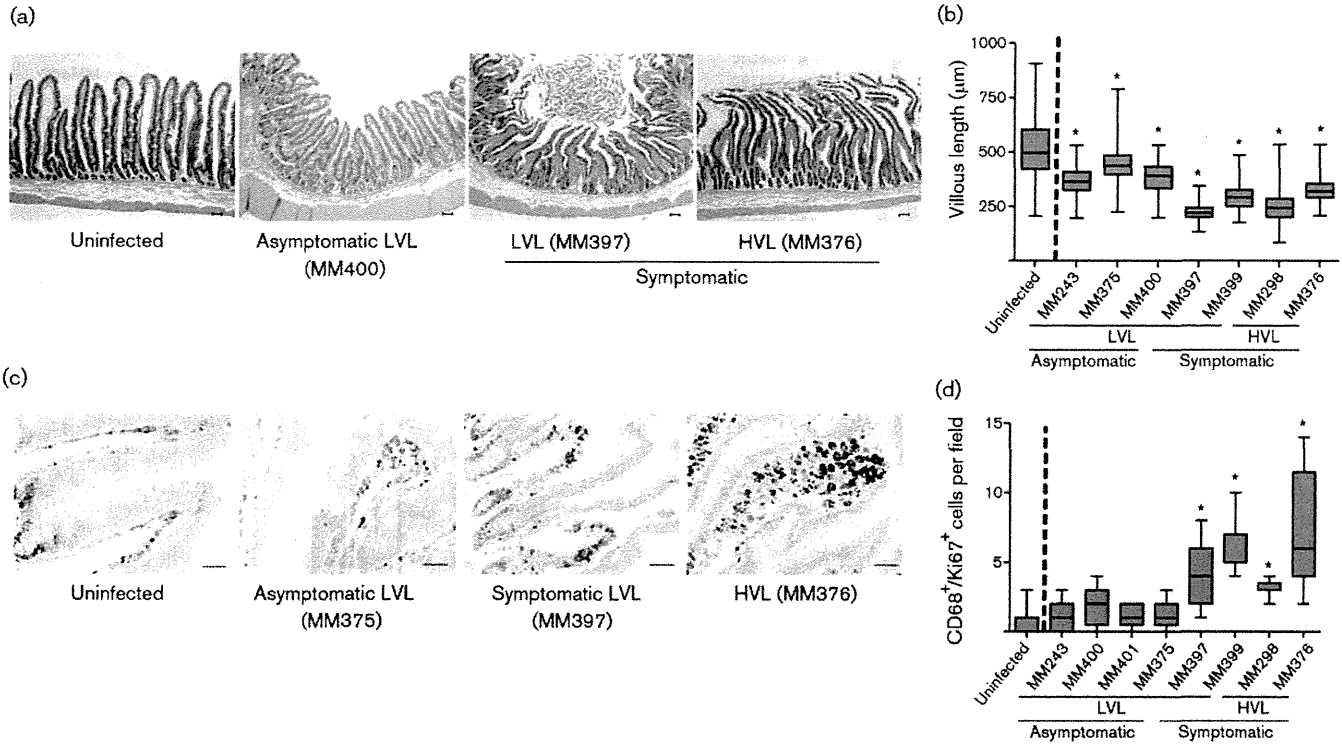

Fig. 3. Villous length in jejunum and counts of activated macrophages in the small intestine at the time of euthanasia in SHIV-KS661-infected rhesus macaques. (a) H&E-stained sections of jejunum of representative uninfected, Asym LVL, Sym LVL and HVL macaques. Bars, 200 μm. (b) Comparison of villous length in uninfected and infected macaques. The lengths of at least 100 villi were measured in each macaque. Statistical analysis was performed using Student's *t*-test for the data from four uninfected and each infected macaque (*, $P<0.0001$). Data for MM299, MM338, MM339 and MM401 were not available. (c) Ki67 and CD68 staining in the small intestine of representative uninfected, Asym LVL, Sym LVL and HVL macaques. Brown staining indicates $Ki67^+$ cells and blue staining indicates $CD68^+$ cells. Bar, 50 μm. (d) Comparison of $CD68^+$ $Ki67^+$ cell counts in uninfected and infected macaques. The numbers of $CD68^+$ $Ki67^+$ cells were enumerated in at least ten fields of the tissues at a magnification of 200×. Statistical analysis was performed using Student's *t*-test for the data from seven uninfected and each infected macaque (*, $P<0.0001$). Data for MM299, MM338 and MM339 were not available.

an LVL. The LVL macaques had much stronger antibody responses than the HVL macaques (Table 1). SHIV-89.6P is easily controlled by the antibody response (Montefiori *et al.*, 1998). SHIV-KS661, which shares its genetic origin with SHIV-89.6P, might be strongly affected by the antibody response. Virus replication during the primary phase clearly occurred later in the intrarectally inoculated macaques than in the intravenously inoculated macaques. Therefore, this delay might contribute to the continuous and strong antibody response in the intrarectally inoculated macaques, consequently resulting in a low viral load in most of the intrarectally inoculated macaques.

The purpose of this study was to elucidate why LVL macaques experience diarrhoea and wasting. A comparison of circulating $CD4^+$ T-cell counts (Fig. 2a) and relative levels of naïve T-cells (Fig. 2b) in LVL macaques did not reveal a substantial difference between Sym LVL (which showed diarrhoea and wasting) and Asym LVL (which were healthy) macaques. The villous length in the intestine also did not affect the level of malignancy of the disease condition, as all infected monkeys showed significant villous atrophy, suggesting a high sensitivity to infection itself. However, Sym LVL and HVL macaques exhibited two findings that Asym LVL macaques did not: (i) $CD4^+$ cell reduction in intestinal and lymphoid tissues (Fig. 2c, d), a hallmark of AIDS; and (ii) abnormal innate immune activation, which was reflected by an increased number of activated macrophages within the intestines (Fig. 3c, d). Ki67 serves as a proliferation marker and proliferation of macrophages may seem unlikely. However, there are some reports about local macrophage proliferation in inflammation sites, indicating the infiltration of activated macrophages associated with tissue damage (Isbel *et al.*, 2001; Norton, 1999). These observations indicated the existence of immunopathological disorders in the intestines not only in HVL macaques but also in Sym LVL macaques.

Many studies have shown positive correlations between the development of AIDS and some characteristic features in

the intestinal tracts of HIV-1-infected humans and pathogenic SIV- or SHIV-infected monkeys: continuous $CD4^+$ T-cell depletion (Brenchley *et al.*, 2004; Ling *et al.*, 2007), abnormal and chronic immune activation (Brenchley *et al.*, 2006; Hazenberg *et al.*, 2003) and enteropathy (Kotler, 2005). Immune activation (as shown by an increased number of intestinal activated macrophages) and intestinal $CD4^+$ cell depletion in Sym LVL macaques strongly suggest the presence of an AIDS-like disease in this subset of animals. Hence, these results suggest that an AIDS-like intestinal disease can occur in LVL macaques despite their low viral load, as well as in HVL macaques.

Some HIV-1-infected patients experience poor recovery of circulating $CD4^+$ T cells, even when their plasma HIV-1 RNA load is suppressed by HAART (Kaufmann *et al.*, 2003; Marchetti *et al.*, 2006; Piketty *et al.*, 1998). These individuals are called immunological non-responders (Marchetti *et al.*, 2006), and have been found to have increased plasma lipopolysaccharide levels, suggesting that bacteria had been translocated from the intestines into the circulation with concomitant activation of T-cell compartments (Marchetti *et al.*, 2006, 2008). Furthermore, some patients who maintain an undetectable or nearly undetectable plasma viral RNA load in the absence of HAART also develop AIDS disease progression (Madec *et al.*, 2005) and have abnormal immune activation and increased plasma lipopolysaccharide levels (Hunt *et al.*, 2008). These observations may indicate that disease progression in a subset of HIV-1-infected individuals is independent of viraemia. Accordingly, the disease progression under conditions of low viral load that we observed in SHIV-KS661-infected macaques can also occur in HIV-1-infected individuals.

Consistent with the fact that intestinal $CD4^+$ cell depletion triggers mucosal immune dysfunction, a notable difference observed between Sym LVL and Asym LVL macaques was the low $CD4^+$ cell frequency in the intestines of the Sym LVL macaques. We propose that the intestinal $CD4^+$ cells in Sym LVL macaques were not able to recover after intestinal $CD4^+$ cell reduction during the early phases of infection. We reported previously that SHIV-KS661 infection of rhesus macaques caused early intestinal $CD4^+$ T-cell depletion (Fukazawa *et al.*, 2008; Miyake *et al.*, 2006). Although we did not examine the macaques during the early phases of infection, the intestinal $CD4^+$ T cells of both Sym LVL and Asym LVL macaques should have been depleted at this time, as even moderately pathogenic SHIV can cause intestinal $CD4^+$ cell reduction during the early phase of infection (Fukazawa *et al.*, 2008). Therefore, the near-normal frequency of intestinal $CD4^+$ cells in Asym LVL macaques would be the result of $CD4^+$ cell recovery after intestinal $CD4^+$ cell reduction during the early phase of infection. In contrast, intestinal $CD4^+$ cells in Sym LVL macaques may be unable to recover, even though virus replication has been controlled. Similarly, intestinal $CD4^+$ cell recovery was found to be important for halting disease progression in SIVmac239-infected rhesus macaques (Ling *et al.*, 2007). Accordingly, one of the important determinants for disease progression in SHIV-KS661-infected macaques may be $CD4^+$ cell recovery in the intestines.

We further hypothesize that this inappropriately low level of $CD4^+$ cells within the intestines of the SHIV-KS661-infected animals (and phenotypically similar humans) is permissive to the excessive activation of resident tissue macrophages. One implication of these studies is that regulatory T-cell subsets of $CD4^+$ cells may be especially vulnerable to this depletion, thus allowing this macrophage activation in view of the well-known role of regulatory T cells in inhibiting innate immune responses (Maloy *et al.*, 2003). This hypothesis will be important to assess in future studies to understand the pathophysiology in the intestines during the chronic phase of HIV-1 infection.

Taken together, the present results suggest that $CD4^+$ cell reduction and enteropathy can occur in SHIV-KS661-infected rhesus macaques even when the viral load is low. The ability or inability to restore intestinal $CD4^+$ cells may be a key factor determining disease progression, irrespective of virus replication levels in the chronic phase of SHIV-KS661 infection. The reason that the recovery of intestinal $CD4^+$ cells is impeded is unknown, although we can speculate on some possibilities such as the co-existence of other infectious microbial agents or impaired T-cell reconstitution caused by damage during thymopoiesis at an early phase of SHIV infection (Motohara *et al.*, 2006). We demonstrated comparable proviral DNA loads in the examined tissues between Sym and Asym LVL macaques, although the $CD4^+$ cell frequencies in the tissues were clearly reduced in Sym LVL macaques. Therefore, the quantity of provirus per CD4 cell in the tissues of Sym LVL macaques is considered to be relatively higher than that of Asym LVL macaques, and low-level replication that may be undetectable in the plasma viral load might be maintained in Sym LVL but not in Asym LVL macaques. Identifying the mechanisms of poor recovery of intestinal $CD4^+$ cells is needed to understand AIDS pathogenesis, because, as stated above, some HIV-1-infected patients have low $CD4^+$ T-cell counts even when viraemia is controlled. One useful approach is comparative and periodical analysis, including cellular immunology data, of the intestinal tract of the same animals from the early to the chronic phases using Sym LVL and Asym LVL macaques in this SHIV infection macaque model.

METHODS

Virus, animals and sample collection. Highly pathogenic SHIV-KS661 is a molecular clone of SHIV-C2/1 (GenBank accession no. AF217181), which was derived through *in vivo* passages of SHIV-89.6 (Shinohara *et al.*, 1999). The virus stock was prepared from the supernatant of virus-infected CEMx174 and M8166 human lymphoid cell lines.

All rhesus macaques used in this study were treated in accordance with the institutional regulations approved by the Committee for

Experimental Use of Non-human Primates in the Institute for Virus Research, Kyoto University, Japan. All macaques were inoculated with 2×10^3 50 % tissue culture infectious dose of SHIV-KS661 measured with CEMx174. The animal ID numbers, infection route and when they were euthanized are provided in Fig. 1(a).

Blood was collected periodically using sodium citrate as an anti-coagulant and examined by flow cytometry and for quantification of plasma viral RNA load. Tissue samples were obtained at the time of euthanasia and were used for quantification of proviral DNA and histopathology.

Determination of plasma viral RNA and proviral DNA loads. The viral loads in plasma and proviral DNA loads in lymphoid and intestinal tissues were determined by quantitative RT-PCR and quantitative PCR, respectively, as described previously (Motohara *et al.*, 2006). DNA samples were extracted directly from frozen tissue sections of each monkey using a DNeasy Tissue kit (Qiagen) according to the manufacturer's protocol.

Determination of antibody titres. Anti-HIV antibody titres were determined using a commercial particle agglutination kit (Serodia-HIV1/2; Fujirebio). Isolated plasma samples were serially diluted and assayed. The end point of the highest dilution giving a positive result was determined as the titre.

Flow cytometry. Flow cytometry was performed as described previously (Motohara *et al.*, 2006). Briefly, $CD4^+$ T cells were analysed by a combination of fluorescein isothiocyanate (FITC)-conjugated anti-monkey CD3 (clone FN-18; BioSource) and phycoerythrin-conjugated anti-human CD4 (clone NU-TH/I; Nichirei), and subsets of naïve and memory $CD4^+$ cells were analysed by a combination of FITC-conjugated anti-human CD95 (clone DX2; BD Pharmingen) and allophycocyanin-conjugated anti-human CD4 (clone L200; BD Pharmingen). $CD95^-$ $CD4^+$ cells were defined as naïve $CD4^+$ T cells and $CD95^+$ $CD4^+$ cells were defined as memory $CD4^+$ T cells. Labelled lymphocytes were examined on a FACSCalibur analyser using CellQuest software (BD Biosciences).

Histology and immunohistochemistry. Tissue samples were fixed in 4 % paraformaldehyde in PBS at 4 °C overnight and embedded in paraffin wax. Sections (4 μm) were dewaxed using xylene, rehydrated through an alcohol gradient, and stained with H&E. The villous length of the jejunum was measured with a micrometer. At least 40 villi from each section were measured.

For immunohistochemistry, sections were rehydrated and processed for 10 min in an autoclave in 10 mM citrate buffer (pH 6.0) to unmask the antigens, sequentially treated with TBS/Tween 20 (TBST) and aqueous hydrogen peroxide, left at 4 °C overnight or at room temperature for 30 min or 1 h for primary antibody reactions, washed with TBST, incubated at room temperature for 1 h with an Envision+ kit (a horseradish peroxidase-labelled anti-mouse immunoglobulin polymer; Dako), visualized using diaminobenzidine (DAB) substrate (Dako) as a chromogen, rinsed in distilled water, counterstained with haematoxylin and analysed by light microscopy (Biozero BZ-8000: Keyence).

For double staining (CD68 and Ki67) of sections, appropriately processed sections were incubated at room temperature for 1 h with unlabelled anti-Ki67 antibody at a dilution of 1 : 2000, the highly sensitive tyramide amplification step (CSAII; Dako) was performed, the slides were reacted with DAB to visualize the results and incubated with unlabelled anti-CD68 antibody at 4 °C overnight followed by incubation at room temperature for 1 h with Histofine Simple Stain AP (an alkaline phosphatase-labelled anti-mouse immunoglobulin polymer (Nichirei), and the results were visualized with a Blue Alkaline Phosphatase Substrate kit III (Vector Laboratories). Measurements of $CD68^+$ $Ki67^+$ cell counts were performed in ten fields at a magnification of 200 × by light microscopy.

Primary antibodies used in immunohistochemistry were anti-human CD4 (diluted 1 : 30; clone NCL-CD4; Novacastra Laboratories), anti-SIV Nef (diluted 1 : 500; FIT Biotech), anti-human CD68 (diluted 1 : 50; clone KP-1; Dako) and anti-human Ki67 (Ki-S5; Dako).

Statistical analysis. The significance of $CD4^+$ or $CD68^+$ $Ki67^+$ cell frequency measurements and villous length in the jejunum of infected monkeys compared with uninfected monkeys was analysed using an unpaired Student's *t*-test (two-tailed) using GraphPad Prism 4.0E software (Varsity Wave).

ACKNOWLEDGEMENTS

We are grateful to Dr James Raymond for editing the English of this manuscript; to Takahito Kazama, Reii Horiuchi, Noriko Nakajima and Tetsutaro Sata for technical support; to Dr Michael A. Eckhaus for histopathological interpretation; and to Takeshi Kobayashi for critical reading. This work was supported, in part, by Research on HIV/AIDS in Health and Labour Sciences Research Grants from the Ministry of Health, Labour and Welfare, Japan; a Grant-in-Aid for Scientific Research from the Ministry of Education and Science, Japan; a Research Grant for AIDS on Health Sciences focusing on Drug Innovation from the Japan Health Sciences Foundation; and a Program for the Promotion of Fundamental Studies in Health Sciences of the National Institute of Biomedical Innovation (NIBIO) of Japan.

REFERENCES

Anton, P. A., Elliott, J., Poles, M. A., McGowan, I. M., Matud, J., Hultin, L. E., Grovit-Ferbas, K., Mackay, C. R., Chen, I. S. Y. & Giorgi, J. V. (2000). Enhanced levels of functional HIV-1 co-receptors on human mucosal T cells demonstrated using intestinal biopsy tissue. *AIDS* **14**, 1761–1765.

Batman, P. A., Miller, A. R., Forster, S. M., Harris, J. R., Pinching, A. J. & Griffin, G. E. (1989). Jejunal enteropathy associated with human immunodeficiency virus infection: quantitative histology. *J Clin Pathol* **42**, 275–281.

Brenchley, J. M., Schacker, T. W., Ruff, L. E., Price, D. A., Taylor, J. H., Beilman, G. J., Nguyen, P. L., Khoruts, A., Larson, M. & other authors (2004). $CD4^+$ T cell depletion during all stages of HIV disease occurs predominantly in the gastrointestinal tract. *J Exp Med* **200**, 749–759.

Brenchley, J. M., Price, D. A., Schacker, T. W., Asher, T. E., Silvestri, G., Rao, S., Kazzaz, Z., Bornstein, E., Lambotte, O. & other authors (2006). Microbial translocation is a cause of systemic immune activation in chronic HIV infection. *Nat Med* **12**, 1365–1371.

Fackler, O. T., Schafer, M., Schmidt, W., Zippel, T., Heise, W., Schneider, T., Zeitz, M., Riecken, E. O., Mueller-Lantzsch, N. & Ullrich, R. (1998). HIV-1 p24 but not proviral load is increased in the intestinal mucosa compared with the peripheral blood in HIV-infected patients. *AIDS* **12**, 139–146.

Fukazawa, Y., Miyake, A., Ibuki, K., Inaba, K., Saito, N., Motohara, M., Horiuchi, R., Himeno, A., Matsuda, K. & other authors (2008). Small intestine $CD4^+$ T cells are profoundly depleted during acute simian–human immunodeficiency virus infection, regardless of viral pathogenicity. *J Virol* **82**, 6039–6044.

Gibbons, T. & Fuchs, G. J. (2007). Chronic enteropathy: clinical aspects. *Nestle Nutr Workshop Ser Pediatr Program* **59**, 89–101.

Hazenberg, M. D., Otto, S. A., van Benthem, B. H., Roos, M. T., Coutinho, R. A., Lange, J. M., Hamann, D., Prins, M. & Miedema, F.

(2003). Persistent immune activation in HIV-1 infection is associated with progression to AIDS. *AIDS* **17**, 1881–1888.

Hunt, P. W., Brenchley, J., Sinclair, E., McCune, J. M., Roland, M., Page-Shafer, K., Hsue, P., Emu, B., Krone, M. & other authors (2008). Relationship between T cell activation and $CD4^+$ T cell count in HIV-seropositive individuals with undetectable plasma HIV RNA levels in the absence of therapy. *J Infect Dis* **197**, 126–133.

Isbel, N. M., Nikolic-Paterson, D. J., Hill, P. A., Dowling, J. & Atkins, R. C. (2001). Local macrophage proliferation correlates with increased renal M-CSF expression in human glomerulonephritis. *Nephrol Dial Transplant* **16**, 1638–1647.

Kahn, E. (1997). Gastrointestinal manifestations in pediatric AIDS. *Pediatr Pathol Lab Med* **17**, 171–208.

Kaufmann, G. R., Perrin, L., Pantaleo, G., Opravil, M., Furrer, H., Telenti, A., Hirschel, B., Ledergerber, B., Vernazza, P. & other authors (2003). CD4 T-lymphocyte recovery in individuals with advanced HIV-1 infection receiving potent antiretroviral therapy for 4 years: the Swiss HIV Cohort Study. *Arch Intern Med* **163**, 2187–2195.

Kotler, D. P. (2005). HIV infection and the gastrointestinal tract. *AIDS* **19**, 107–117.

Lapenta, C., Boirivant, M., Marini, M., Santini, S. M., Logozzi, M., Viora, M., Belardelli, F. & Fais, S. (1999). Human intestinal lamina propria lymphocytes are naturally permissive to HIV-1 infection. *Eur J Immunol* **29**, 1202–1208.

Ling, B., Veazey, R. S., Hart, M., Lackner, A. A., Kuroda, M., Pahar, B. & Marx, P. A. (2007). Early restoration of mucosal CD4 memory CCR5 T cells in the gut of SIV-infected rhesus predicts long term non-progression. *AIDS* **21**, 2377–2385.

Madec, Y., Boufassa, F., Porter, K. & Meyer, L. (2005). Spontaneous control of viral load and CD4 cell count progression among HIV-1 seroconverters. *AIDS* **19**, 2001–2007.

Maloy, K. J., Salaun, L., Cahill, R., Dougan, G., Saunders, N. J. & Powrie, F. (2003). $CD4^+CD25^+$ T_R cells suppress innate immune pathology through cytokine-dependent mechanisms. *J Exp Med* **197**, 111–119.

Marchetti, G., Gori, A., Casabianca, A., Magnani, M., Franzetti, F., Clerici, M., Perno, C. F., Monforte, A., Galli, M. & Meroni, L. (2006). Comparative analysis of T-cell turnover and homeostatic parameters in HIV-infected patients with discordant immune-virological responses to HAART. *AIDS* **20**, 1727–1736.

Marchetti, G., Bellistri, G. M., Borghi, E., Tincati, C., Ferramosca, S., La Francesca, M., Morace, G., Gori, A. & Monforte, A. D. (2008). Microbial translocation is associated with sustained failure in $CD4^+$ T-cell reconstitution in HIV-infected patients on long-term highly active antiretroviral therapy. *AIDS* **22**, 2035–2038.

Miyake, A., Ibuki, K., Enose, Y., Suzuki, H., Horiuchi, R., Motohara, M., Saito, N., Nakasone, T., Honda, M. & other authors (2006). Rapid dissemination of a pathogenic simian/human immunodeficiency virus to systemic organs and active replication in lymphoid tissues following intrarectal infection. *J Gen Virol* **87**, 1311–1320.

Montefiori, D. C., Reimann, K. A., Wyand, M. S., Manson, K., Lewis, M. G., Collman, R. G., Sodroski, J. G., Bolognesi, D. P. & Letvin, N. L. (1998). Neutralizing antibodies in sera from macaques infected with chimeric simian–human immunodeficiency virus containing the envelope glycoproteins of either a laboratory-adapted variant or a primary isolate of human immunodeficiency virus type 1. *J Virol* **72**, 3427–3431.

Motohara, M., Ibuki, K., Miyake, A., Fukazawa, Y., Inaba, K., Suzuki, H., Masuda, K., Minato, N., Kawamoto, H. & other authors (2006). Impaired T-cell differentiation in the thymus at the early stages of acute pathogenic chimeric simian–human immunodeficiency virus (SHIV) infection in contrast to less pathogenic SHIV infection. *Microbes Infect* **8**, 1539–1549.

Norton, W. T. (1999). Cell reactions following acute brain injury: a review. *Neurochem Res* **24**, 213–218.

Paiardini, M., Frank, I., Pandrea, I., Apetrei, C. & Silvestri, G. (2008). Mucosal immune dysfunction in AIDS pathogenesis. *AIDS Rev* **10**, 36–46.

Piketty, C., Castiel, P., Belec, L., Batisse, D., Si Mohamed, A., Gilquin, J., Gonzalez-Canali, G., Jayle, D., Karmochkine, M. & other authors (1998). Discrepant responses to triple combination antiretroviral therapy in advanced HIV disease. *AIDS* **12**, 745–750.

Sestak, K. (2005). Chronic diarrhea and AIDS: insights into studies with non-human primates. *Curr HIV Res* **3**, 199–205.

Sharpstone, D. & Gazzard, B. (1996). Gastrointestinal manifestations of HIV infection. *Lancet* **348**, 379–383.

Shinohara, K., Sakai, K., Ando, S., Ami, Y., Yoshino, N., Takahashi, E., Someya, K., Suzaki, Y., Nakasone, T. & other authors (1999). A highly pathogenic simian/human immunodeficiency virus with genetic changes in cynomolgus monkey. *J Gen Virol* **80**, 1231–1240.

Smith, P. D., Meng, G., Salazar-Gonzalez, J. F. & Shaw, G. M. (2003). Macrophage HIV-1 infection and the gastrointestinal tract reservoir. *J Leukoc Biol* **74**, 642–649.

Veazey, R. S., DeMaria, M., Chalifoux, L. V., Shvetz, D. E., Pauley, D. R., Knight, H. L., Rosenzweig, M., Johnson, R. P., Desrosiers, R. C. & Lackner, A. A. (1998). Gastrointestinal tract as a major site of $CD4^+$ T cell depletion and viral replication in SIV infection. *Science* **280**, 427–431.

Veazey, R. S., Mansfield, K. G., Tham, I. C., Carville, A. C., Shvetz, D. E., Forand, A. E. & Lackner, A. A. (2000a). Dynamics of CCR5 expression by $CD4^+$ T cells in lymphoid tissues during simian immunodeficiency virus infection. *J Virol* **74**, 11001–11007.

Veazey, R. S., Tham, I. C., Mansfield, K. G., DeMaria, M., Forand, A. E., Shvetz, D. E., Chalifoux, L. V., Sehgal, P. K. & Lackner, A. A. (2000b). Identifying the target cell in primary simian immunodeficiency virus (SIV) infection: highly activated memory $CD4^+$ T cells are rapidly eliminated in early SIV infection in vivo. *J Virol* **74**, 57–64.

Wilcox, C. M. & Saag, M. S. (2008). Gastrointestinal complications of HIV infection: changing priorities in the HAART era. *Gut* **57**, 861–870.

JOURNAL OF VIROLOGY, May 2010, p. 4769–4781 Vol. 84, No. 9
0022-538X/10/$12.00 doi:10.1128/JVI.02279-09

Generation of the Pathogenic R5-Tropic Simian/Human Immunodeficiency Virus $SHIV_{AD8}$ by Serial Passaging in Rhesus Macaques[▽]†

Yoshiaki Nishimura,[1] Masashi Shingai,[1] Ronald Willey,[1] Reza Sadjadpour,[1] Wendy R. Lee,[1] Charles R. Brown,[1] Jason M. Brenchley,[1] Alicia Buckler-White,[1] Rahel Petros,[2] Michael Eckhaus,[3] Victoria Hoffman,[3] Tatsuhiko Igarashi,[1]‡ and Malcolm A. Martin[1]*

Laboratory of Molecular Microbiology[1] and Comparative Medicine Branch,[2] National Institute of Allergy and Infectious Diseases, and Diagnostic and Research Services Branch, Division of Veterinary Resources, Office of the Director,[3] National Institutes of Health, Bethesda, Maryland 20892

Received 28 October 2009/Accepted 31 January 2010

A new pathogenic R5-tropic simian/human immunodeficiency virus (SHIV) was generated following serial passaging in rhesus macaques. All 13 animals inoculated with $SHIV_{AD8}$ passaged lineages experienced marked depletions of $CD4^+$ T cells. Ten of these infected monkeys became normal progressors (NPs) and had gradual losses of both memory and naïve $CD4^+$ T lymphocytes, generated antiviral $CD4^+$ and $CD8^+$ T cell responses, and sustained chronic immune activation while maintaining variable levels of plasma viremia (10^2 to 10^5 RNA copies/ml for up to 3 years postinfection [p.i.]). To date, five NPs developed AIDS associated with opportunistic infections caused by *Pneumocystis carinii*, *Mycobacterium avium*, and *Campylobacter coli* that required euthanasia between weeks 100 and 199 p.i. Three other NPs have experienced marked depletions of circulating $CD4^+$ T lymphocytes (92 to 154 cells/μl) following 1 to 2 years of infection. When tested for coreceptor usage, the viruses isolated from four NPs at the time of their euthanasia remained R5 tropic. Three of the 13 $SHIV_{AD8}$-inoculated macaques experienced a rapid-progressor syndrome characterized by sustained plasma viremia of $>1 \times 10^7$ RNA copies/ml and rapid irreversible loss of memory $CD4^+$ T cells that required euthanasia between weeks 19 and 23 postinfection. The sustained viremia, associated depletion of $CD4^+$ T lymphocytes, and induction of AIDS make the $SHIV_{AD8}$ lineage of viruses a potentially valuable reagent for vaccine studies.

Simian immunodeficiency virus (SIV)/macaque models of AIDS have been extensively used as surrogates for human immunodeficiency virus type 1 (HIV-1) in studies of virus-induced immunopathogenesis and vaccine development. As is observed for the HIVs recovered from a majority of individuals during the asymptomatic phase of their infections, pathogenic SIVs utilize the CCR5 coreceptor to enter their $CD4^+$ T lymphocyte targets *in vivo* (36). This leads to the elimination of memory $CD4^+$ T cells circulating in the blood and residing at effector sites (gastrointestinal [GI] tract, mucosal surfaces, and lung), particularly during acute HIV and SIV infections (5, 29, 32, 49). In contrast to naturally occurring SIVs and HIVs, SIV/HIV chimeric viruses (simian/human immunodeficiency viruses [SHIVs]) were constructed in the laboratory by inserting a large segment of the HIV genome, including the *env* gene, into the genetic backbone of the molecularly cloned SIV_{mac239} (44). SHIVs were developed because they expressed the HIV envelope glycoprotein and could be used in vaccine experiments to evaluate neutralizing antibodies (NAbs) elicited by HIV-1 gp120 immunogens. The commonly used pathogenic SHIVs generated high levels (10^7 to 10^8 RNA copies/ml) of plasma viremia and induced an extremely rapid, systemic, and nearly complete depletion of the entire $CD4^+$ T cell population, resulting in death from immunodeficiency beginning at 3 months postinoculation (23, 26, 41). Unlike SIVs, however, these pathogenic SHIVs exclusively targeted CXCR4-expressing $CD4^+$ T cells during infections of rhesus monkeys (36). Despite their extraordinary virulence, most vaccine regimens (naked DNA, peptides, proteins, inactivated virions, recombinant modified vaccinia virus Ankara (MVA), and DNA prime/recombinant viral-vector boosting) were effective in controlling intravenous (i.v.) and mucosal X4-tropic SHIV challenges (1, 3, 33, 42, 46). When it became apparent that the same vaccination strategies that were effective in suppressing pathogenic SHIVs failed to control SIV infections, concerns were raised about whether X4 SHIVs were appropriate surrogates for HIV in vaccine experiments (13).

The unusual biological properties of the X4 SHIVs plus the discrepant outcomes of SIV and X4 SHIV vaccine experiments have become a driving force for developing CCR5-utilizing (R5) SHIVs. Although several clade B and clade C R5-tropic SHIVs have been constructed (7, 15, 21, 30, 38), the $SHIV_{SF162}$ lineage viruses are the best-characterized and most widely used R5 SHIVs (20). They have been employed in microbicide (10), neutralizing monoclonal antibody (MAb) passive-transfer (16, 17), and vaccination (2) studies.

* Corresponding author. Mailing address: Bldg. 4, Room 315A, 4 Center Drive MSC 0460, National Institutes of Health, Bethesda, MD 20892-0460. Phone: (301) 496-4012. Fax: (301) 402-0226. E-mail: malm@nih.gov.

‡ Present address: Laboratory of Primate Models, Institute for Virus Research, Kyoto University, 53 Shogoinkawaramachi, Sakyo-ku, Kyoto 606-8507, Japan.

† Supplemental material for this article may be found at http://jvi.asm.org/.

▽ Published ahead of print on 10 February 2010.

In the aftermath of the failed STEP HIV vaccine trial, there was general consensus that additional SIVs and SHIVs should be developed, particularly for use as heterologous challenge viruses in vaccine studies (12). With this goal in mind, we report the generation of a new pathogenic R5-tropic SHIV bearing the *env* gene from the HIV-1_{Ada} isolate (14). HIV-1_{Ada} was selected because it is a prototypical macrophage-tropic strain (8), uses CCR5 for cell entry (53), and has the potential for eliciting NAbs against HIV-1 gp120, and we had previously constructed a full-length infectious molecular clone (pHIV-1_{AD8}) (48). Based on previous experience in obtaining pathogenic X4-tropic SHIVs, serial passaging in macaques, treated with an anti-CD8 MAb at the time of virus inoculation, was used to expedite the adaptation of R5-SHIV sequences in a nonhuman primate host. Of the 13 animals inoculated with *in vivo*-passaged $SHIV_{AD8\#2}$ (see below) and its immediate derivatives, 10 exhibited a normal-progressor (NP) phenotype, sustaining gradual depletions of both memory and naïve $CD4^+$ T cells from the circulation and memory $CD4^+$ T cells at an effector site (lung) while maintaining variable viral-RNA loads (10^2 to 10^5 RNA copies/ml) for up to 3 years postinfection (p.i.). Five of these monkeys developed immunodeficiency with associated opportunistic infections requiring euthanasia. Three other NPs currently have total $CD4^+$ T cell counts of 92 to 154 cells/μl plasma after 1 to 2 years of infection. The remaining 3 of the 13 $SHIV_{AD8}$-inoculated macaques experienced a rapid-progressor (RP) clinical course and were euthanized between weeks 19 and 23 p.i. because of intractable diarrhea and marked weight loss. The sustained viremia, associated depletion of $CD4^+$ T lymphocytes, and induction of AIDS make the $SHIV_{AD8}$ lineage of viruses a potentially valuable reagent for vaccine studies.

TABLE 1. Infection of rhesus macaques with $SHIV_{AD8\#2}$ and immediate derivatives

Animal	Inoculum
CJ8B	$SHIV_{AD8\#2}$
CK15	Blood transfusion from CJ8B (wk 60)
CJ58	Blood transfusion from CJ8B (wk 60)
CE8J	Lymph node virus[a] ($SHIV_{AD8\#2LN}$, 3.2×10^5 $TCID_{50}$) from CJ8B (wk 59)
CJ35	Lymph node virus ($SHIV_{AD8\#2LN}$, 3.2×10^5 $TCID_{50}$) from CJ8B (wk 59)
CJ3V	PBMC virus[b] ($SHIV_{AD8\#2PBMC}$, 5.9×10^4 $TCID_{50}$) from CK15 + CJ58 (wk 4)
CK5G	PBMC virus ($SHIV_{AD8\#2PBMC}$, 5.9×10^4 $TCID_{50}$) from CK15 + CJ58 (wk 4)
DB99	Blood transfusion from CJ8B (wk 117) + CK15 (wk 57) + CJ58 (wk 57)
DA1Z	Blood transfusion from CJ8B (wk 117) + CK15 (wk 57) + CJ58 (wk 57)
A4E008	Blood transfusion from DA1Z (wk 1) + DB99 (wk 1)
DA4W	Blood transfusion from DA1Z (wk 1) + DB99 (wk 1)
CL5A	$SHIV_{AD8\#2}$ passaged *in vitro* for 30 days ($SHIV_{AD8\#2.d30}$, 4.3×10^5 $TCID_{50}$)
CL98	SHIVAD8#2 passaged *in vitro* for 30 days ($SHIV_{AD8\#2.d30}$, 4.3×10^5 $TCID_{50}$)

[a] Lymph node virus: $SHIV_{AD8}$ derivative prepared from the supernatant medium collected from cocultures of lymph node suspensions plus PBMC, recovered from animal CJ8B at week 59 p.i., and PBMC from uninfected rhesus monkeys.

[b] PBMC virus: $SHIV_{AD8}$ derivative prepared from the supernatant medium collected from cocultures of PBMC, recovered from the indicated infected animals at week 4 p.i., and PBMC from uninfected rhesus monkeys.

MATERIALS AND METHODS

Construction of $SHIV_{AD8}$. $SHIV_{AD8}$ contains the *env* gene from the R5-tropic HIV-1_{Ada} (14)-derived molecular clone $pHIV_{AD8}$ (48). A 3.04-kb segment from $pHIV_{AD8}$, including a portion of the *vpr* gene and the entire *tat*, *rev*, *vpu*, and *env* genes, was PCR amplified using the forward primer TGAAACTTATGGGGA TACTTGGGC, which begins at nucleotide 141 of the AD8 *vpr* gene, allowing the incorporation of a unique EcoRI site, located 21 nucleotides downstream from the primer, into the PCR product. The reverse PCR primer (TCCACCCATAA GCTTATAGCAAAGTCCTTTCCAAGCCC) generated a HindIII site adjacent to and encompassing the last 2 nucleotides of the *env* reading frame, as well as a substitution of a Thr for a Leu 3 codons upstream from the *env* termination codon. PCRs were performed using 10 pmol each of the forward and reverse primers, Platinum PCR SuperMix High Fidelity (Invitrogen), and 1 μl of $pHIV_{AD8}$ in a final volume of 50 μl. The reaction mixtures were heated to 94°C for 2 min, followed by 30 cycles of 94°C for 20 s, 59°C for 30 s, and 70°C for 3 min and a 7-min extension at 70°C. The PCR product was gel extracted using a Qiaquick gel extraction kit (Qiagen) and digested with EcoRI and HindIII, and the resulting 3.04-kb restriction fragment was cloned directly into the previously described and similarly digested $pSHIV_{DH12}$ (45) to generate $pSHIV_{AD8}$. DNA sequencing of the entire 3.04-kb insert in $pSHIV_{AD8}$ was conducted to verify that no spurious changes had been introduced during the PCR amplification and cloning.

Preparation of $SHIV_{AD8}$ virus stocks. HeLa cells were transfected with 25 μg of $pSHIV_{AD8}$, and the virus present in the supernatant at 48 h was pelleted in an ultracentrifuge and resuspended in RPMI 1640 medium as previously described (52). Stocks of the cloned $SHIV_{AD8}$ were prepared by infecting PM1 cells (31) or concanavalin A (ConA)-activated rhesus monkey peripheral blood mononuclear cells (PBMC) with the HeLa-derived $SHIV_{AD8}$, as previously described (23, 24), and pooling the supernatant media at the times of peak reverse transcriptase (RT) production from both infections.

$SHIV_{AD8}$ stock 2 ($SHIV_{AD8\#2}$) was prepared from PBMC and bone marrow (BM), spleen, and lymph node (LN) samples collected from macaque CK1G on day 6 p.i. Cell suspensions from axillary, inguinal, iliac, and mesenteric LNs, PBMC, and BM were cocultivated with PBMC from uninfected animals; the culture supernatants were monitored daily for RT activity, pooled, and designated $SHIV_{AD8\#2}$. The infectious titer of $SHIV_{AD8\#2}$ was 1.5×10^3 tissue culture infective doses ($TCID_{50}$)/ml, as determined in rhesus macaque PBMC.

$SHIV_{AD8}$ lymph node virus ($SHIV_{AD8LN}$) was prepared from supernatant medium collected from cocultures of lymph node suspensions plus PBMC recovered from animal CJ8B at week 59 p.i. (Table 1) and PBMC from uninfected rhesus monkeys. The infectious titer of $SHIV_{AD8LN}$ was 6.4×10^3 $TCID_{50}$/ml, as determined in rhesus macaque PBMC.

$SHIV_{AD8}$ PBMC virus ($SHIV_{AD8PBMC}$) was prepared from supernatant medium collected from cocultures of PBMC recovered and pooled from animals CK15 and CJ58 at week 4 p.i. (Table 1) and PBMC from uninfected rhesus monkeys. The infectious titer of $SHIV_{AD8PBMC}$ was 1.1×10^4 $TCID_{50}$/ml, as determined in rhesus macaque PBMC.

$SHIV_{AD8\#2.d30}$ was prepared by infecting ConA-stimulated pig-tailed macaque (PT) PBMC with $SHIV_{AD8\#2}$. Fresh ConA-stimulated PT PBMC were added to the infected cultures on days 10 and 20, and the supernatant medium collected on day 30, designated $SHIV_{AD8\#2.d30}$, had an infectious titer of 8.5×10^4 $TCID_{50}$/ml, as determined in rhesus macaque PBMC.

Virus replication assay in rhesus monkey PBMC. The preparation and infection of rhesus monkey PBMC have been described previously (25). Briefly, PBMC stimulated with concanavalin A and cultured in the presence of recombinant human interleukin-2 (IL-2) were spinoculated (1,200 × *g* for 1 h) (37) with virus normalized for RT activity. Virus replication was assessed by RT assay of the culture supernatant as described above.

Animal experiments. Rhesus macaques (*Macaca mulatta*) were maintained in accordance with the guidelines of the Committee on Care and Use of Laboratory Animals (9) and were housed in a biosafety level 2 facility; biosafety level 3 practices were followed. Phlebotomies, i.v. virus inoculations, euthanasia, and tissue sample collections were performed as previously described (11). Bronchoalveolar lavage (BAL) fluid lymphocytes were prepared from uninfected and infected animals using a pediatric bronchoscope (Olympus BF3C40; Olympus America, Inc., Melville, NY), as previously described (22).

Serial *in vivo* passaging of $SHIV_{AD8}$ was initiated by transferring whole blood (10 ml) and BM (2 ml) to a recipient animal previously treated with the anti-$CD8^+$ T cell-depleting MAb cM-T807 (10 mg/kg of body weight) on days −1 and +3 p.i. In subsequent passages, spleen, LN (axillary, inguinal, iliac, and mesen-

teric), PBMC, and BM cell suspensions were prepared from infected donors at the time of necropsy and transferred (1×10^8 to 3×10^8 mononuclear cells and 1×10^8 to 10×10^8 BM cells) to a new recipient by the i.v., intraperitoneal (i.p.), and BM routes.

Quantitation of proviral-DNA and plasma viral-RNA levels. The number of viral-DNA copies in PBMC was measured by quantitative DNA PCR (45). Viral-RNA levels in plasma were determined by real-time reverse transcription-PCR (ABI Prism 7700 sequence detection system; Applied Biosystems, Foster City, CA) as previously reported, using reverse-transcribed viral RNA in plasma samples from SIV_{mac239}-inoculated rhesus macaques (11).

Lymphocyte immunophenotyping and data analysis. EDTA-treated blood samples and BAL fluid lymphocytes were stained for flow cytometric analysis as described previously (34, 36), using combinations of the following fluorochrome-conjugated MAbs: CD3 (fluorescein isothiocyanate [FITC] or phycoerythrin [PE]), CD4 (PE, peridinin chlorophyll protein-Cy5.5 [PerCP-Cy5.5], or allophycocyanin [APC]), CD8 (PerCP or APC), CD28 (FITC or PE), CD95 (APC), and Ki-67 (FITC or PE). All antibodies were obtained from BD Biosciences (San Diego, CA), and samples were analyzed by four-color flow cytometry (FACSCalibur; BD Biosciences Immunocytometry Systems). Data analysis was performed using CellQuest Pro (BD Biosciences) and FlowJo (TreeStar, Inc., San Carlos, CA). For Ki-67 staining, cells were fixed with fluorescence-activated cell sorter (FACS) lysing solution (Becton Dickinson), treated with FACS permeabilization buffer 2 (Becton Dickinson), and stained with Ki-67 MAb or a control isotype IgG1. In this study, naïve $CD4^+$ T cells were identified by their $CD95^{low}$ $CD28^{high}$ phenotype, whereas memory $CD4^+$ T cells were $CD95^{high}$ $CD28^{high}$ or $CD95^{high}$ $CD28^{low}$ in the $CD4^+$ small lymphocyte gate (36, 39).

Intracellular-cytokine assays. Stimulation was performed on frozen lymphocytes as described previously (40). Freshly thawed lymphocytes were resuspended (10^6/ml) in RPMI medium supplemented with antibiotics and glutamine. Anti-CD28 conjugated to Alexa 594-PE was used for costimulation. Staphylococcus enterotoxin B (1 μg/ml; Sigma-Aldrich, St. Louis, MO) was used to stimulate T cells mitogenically through the T cell receptor as a positive control. A negative control (cells treated only with costimulatory anti-CD28) was included in every experiment. Peptides used to stimulate SIV-specific T cells were 15 amino acids (aa) in length, overlapping by 11 amino acids, and encompassed SIV_{mac239} Gag (New England Peptide, Gardner, MA). The concentration of each peptide was 2 μg/ml for stimulations, which were performed in the presence of brefeldin A (BFA) (1 μg/ml; Sigma-Aldrich, St. Louis, MO) for 16 h at 37°C. All cells were surface stained with the dead-cell exclusion dye Aqua Blue (Invitrogen Corp., Carlsbad CA), followed by staining with anti-CD3 Alexa 700 (BD Biosciences), anti-CD4 Cy5.5-PE (eBioscience Inc., San Diego, CA), anti-CD8 Pacific Blue (BD Biosciences), and anti-CD95 Cy5-PE (BD Biosciences). The cells were then fixed, permeabilized, and stained with anti-gamma interferon (IFN-γ) Cy7-PE (BD Biosciences), anti-IL-2 APC (BD Biosciences), tumor necrosis factor (TNF) FITC (BD Biosciences), and Mip1-β PE (BD Biosciences). SIV-specific CD8 T cell responses are reported as the frequency of memory CD8 T cells, gated by characteristic light scatter properties; then as Aqua $Blue^-$, $CD3^+$, $CD8^+$, $CD4^-$, or $CD95^+$; and by production of either TNF or Mip-1β. All data are reported after background subtraction.

Virus neutralization assays. Autologous plasma samples (1:20 dilution) from $SHIV_{AD8}$-infected macaques were incubated with (i) the same uncloned $SHIV_{AD8}$ derivative used for inoculation or (ii) the $SHIV_{AD8}$ isolated from PBMC at week 4 p.i. (for monkeys CJ58 and CK15) in quadruplicate in 96-well flat-bottom culture plates in a total volume of 50 μl for 1 h at 37°C. Prechallenge plasma samples from each animal served as controls. Freshly trypsinized TZM-bl cells (50) (1.5×10^4 in 150 μl Dulbecco's modified Eagle's medium [DMEM] containing 20 μg/ml DEAE dextran) were added to each well, and the cultures were maintained in a 37°C incubator for 28 h. The amount of virus-induced luciferase activity, measured as relative light units (RLU), present in cell lysates was determined as previously described (51), and the average neutralization activity for each plasma sample was determined. The average number of RLU for the prechallenge plasma controls ranged from 1×10^5 to 2×10^5. Any sample resulting in a 50% reduction of luciferase activity compared to that obtained with the uninfected control sample was considered positive for NAbs. To determine neutralizing-antibody titers, 40 μl of diluted virus, sufficient to generate the desired numbers of RLU, was mixed with 10 μl of appropriately diluted plasma samples in a 96-well plate and incubated for 1 h at 37°C. TZM-bl cells were added, cultures were maintained for an additional 28 h, and intracellular luciferase activity was measured as described above.

Coreceptor utilization assays. Freshly trypsinized TZM-bl cells (1×10^4 per well) in 135 μl DMEM containing 10% fetal calf serum (FCS) and DEAE dextran (15 μg/ml) were seeded in flat-bottom 96-well plates. Twenty-five microliters of coreceptor antagonists (AD101 against CCR5, AMD3100 against CXCR4, or both, at final concentrations ranging from 0.1 nM to 1,000 nM) was added to each well. Following incubation for 1 h at 37°C, 10 $TCID_{50}$ of replication-competent virus, determined in TZM-bl cells as previously described, in 40 μl was added to each well. After 24 h of incubation at 37°C, luciferase activity was determined. The percent infectivity reported was derived from the mean of quadruplicate assays.

To generate 293T cell-derived $SHIV_{AD8}$ pseudotyped viruses, two separate plasmids were constructed. The first (pNLenv1) contained a frameshifted mutation in the leader peptide region of gp120 (43). Plasmids expressing the $SHIV_{AD8(RIG+)}$ and $SHIV_{AD8(RIG-)}$ *env* genes [pCMV-AD8(RIG+) and AD8(RIG−)] were generated by reverse transcription-PCR of plasma viral RNA, collected from macaque DB99 at the time of euthanasia, and subcloning into NotI and (newly created) XbaI sites of the pCMVbeta expression plasmid (Clonetech, Palo Alto, CA). Both plasmids [pNLenv1 and pCMV-AD8(RIG) in a 5:1 ratio] were cotransfected into 293T cells using Lipofectamine 2000 (Invitrogen, Carlsbad, CA). The titers of pseudotyped-virus preparations were determined, and they were assayed for coreceptor usage 48 h following infection of TZM-bl cells, as described for replication-competent virus.

RESULTS

Construction of a CCR5-tropic SHIV. We previously reported the construction of a full-length infectious HIV-1 molecular clone ($pHIV\text{-}1_{AD8}$) derived from the prototypical macrophage-tropic CCR5-utilizing $HIV\text{-}1_{Ada}$ isolate (14, 48). A SHIV expressing the *env* gene from $pHIV_{AD8}$ was obtained by inserting the 3.04-kb EcoRI-to-HindIII DNA fragment (including a portion of *vpr* and the entire *tat*, *rev*, *vpu*, and *env* genes) into the genetic background of $pSHIV_{DH12}$ (45), as described in Materials and Methods. The resulting molecular clone, $pSHIV_{AD8}$, directed the production of progeny virions following the transfection of HeLa cells. Virus stocks were prepared by infecting PM1 cells or ConA-stimulated rhesus PBMC with virions pelleted from HeLa cell transfection culture supernatants.

It is not generally appreciated how daunting it is to generate an R5-tropic SHIV able to maintain detectable levels of set-point viremia, exclusively target memory $CD4^+$ T cells, and induce immunodeficiency in inoculated rhesus monkeys. Simply replacing orthologous SIV sequences with a DNA segment including a CCR5-utilizing HIV-1 *env* gene does not usually result in a SHIV exhibiting robust replication kinetics *in vivo* and a disease-inducing phenotype. This was, in fact, the case for $SHIV_{AD8}$: levels of plasma viremia following virus inoculation (1 ml of undiluted virus by the i.v., i.p., and BM routes) were promptly and durable suppressed, and the numbers of memory $CD4^+$ T lymphocytes did not change appreciably, as shown for a representative infected animal (CJ7H) in Fig. 1a. To be certain that we were on the right track with respect to the targeting and elimination of memory, not naïve, $CD4^+$ T cells *in vivo*, a second macaque (CJ9F) was treated with the $CD8^+$ T lymphocyte-depleting MAb cM-T807 24 h prior to $SHIV_{AD8}$ inoculation, as well as on days 3 and 6 post-virus infection, to promote a vigorous *in vivo* infection. Unlike untreated macaque CJ7H, the levels of plasma viral RNA in monkey CJ9F rapidly rose to 3.8×10^7 copies/ml by day 10 p.i. and were associated with a rapid and irreversible decline of circulating memory $CD4^+$ T cells (Fig. 1b). In contrast, the numbers of naïve $CD4^+$ T lymphocytes in animal CJ9F were maintained in the 600- to 800-cell/μl range during this period. This result, therefore, confirmed that $SHIV_{AD8}$ could sustain high virus loads and preferentially target the memory $CD4^+$ T

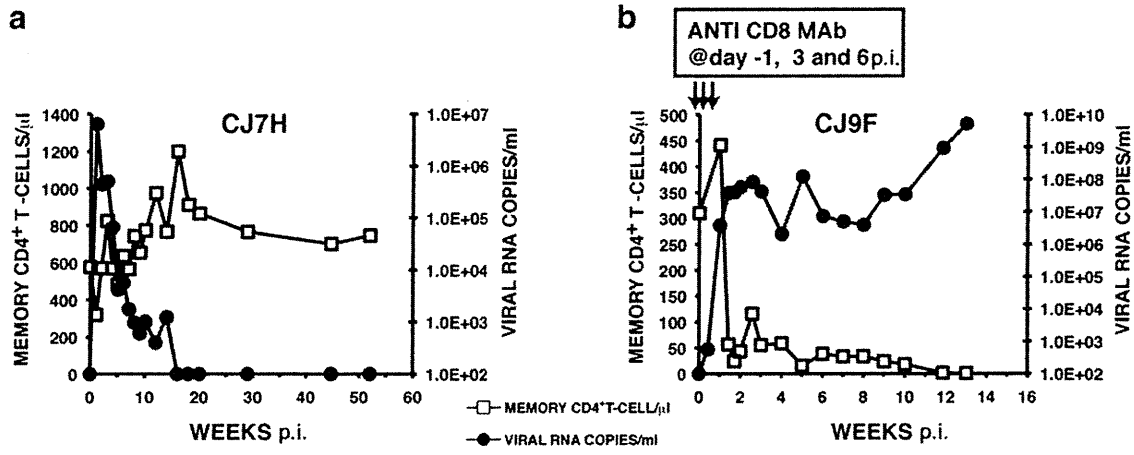

FIG. 1. Infectivity of the original $SHIV_{AD8}$ in rhesus monkeys. Macaques CJ7H (a) and CJ9F (b) were inoculated with 1 ml of undiluted $SHIV_{AD8}$ by the i.v., i.p., and BM routes. Macaque CJ9F was treated with the depleting anti-CD8 MAb cM-T807 as indicated.

cell subset *in vivo*, but only in an animal with a compromised immune system.

***In vivo* passaging of $SHIV_{AD8}$.** The prompt control of plasma viremia and the nonpathogenic phenotype of $SHIV_{AD8}$ observed in untreated macaques were reminiscent of the infectivity patterns observed with first-generation X4-tropic SHIVs (28, 44). We therefore initiated serial animal-to-animal passaging of $SHIV_{AD8}$ with macaque CJ9F as the "founder" infected monkey (Fig. 2a). This approach had previously been used to generate X4 SHIVs exhibiting more robust replicative and pathogenic properties (26, 41). Unfortunately, *in vivo* serial passaging of virus to optimize infectivity is an empirical and stochastic process. One never knows when or if an R5 SHIV has acquired an augmented replicative phenotype. The ultimate proof that such a change has occurred requires the inoculation of additional animals and waiting several months to assess the resultant viral replication kinetics and $CD4^+$ T cell dynamics.

The strategy employed was to maximize the emergence of disease-inducing SHIV variants, putatively present in an increasingly genetically diverse virus population, by serially transferring large numbers of infected cells by i.v., i.p., and BM routes into recipient animals previously treated with an anti-CD8 depleting MAb. As indicated in Fig. 2a, whole blood and bone marrow cells were transferred from macaque CJ9F to macaque H681 by these three routes. In subsequent passages, cell suspensions were prepared from spleen, LN (axillary, inguinal, iliac, and mesenteric), PBMC, and BM cells collected at the time of necropsy, as described in Materials and Methods. With one exception (macaque CJ7F), the depleting anti-CD8 MAb was administered to a recipient animal on days −1 and +3 p.i. to facilitate unrestricted replication *in vivo*. Animal CJ7F did not receive anti-CD8 MAb at the time of virus transfer to investigate the possibility that $SHIV_{AD8}$ had acquired improved replication properties *in vivo* following the initial two *in vivo* passages. Because this was not the case (its plasma viral-RNA loads had declined to 360 RNA copies/ml at week 10 p.i.), macaque CJ7F was treated with anti-CD8 MAb at week 13 p.i. and sustained an immediate burst of virus production that reached 1.4×10^6 RNA copies/ml of plasma at week

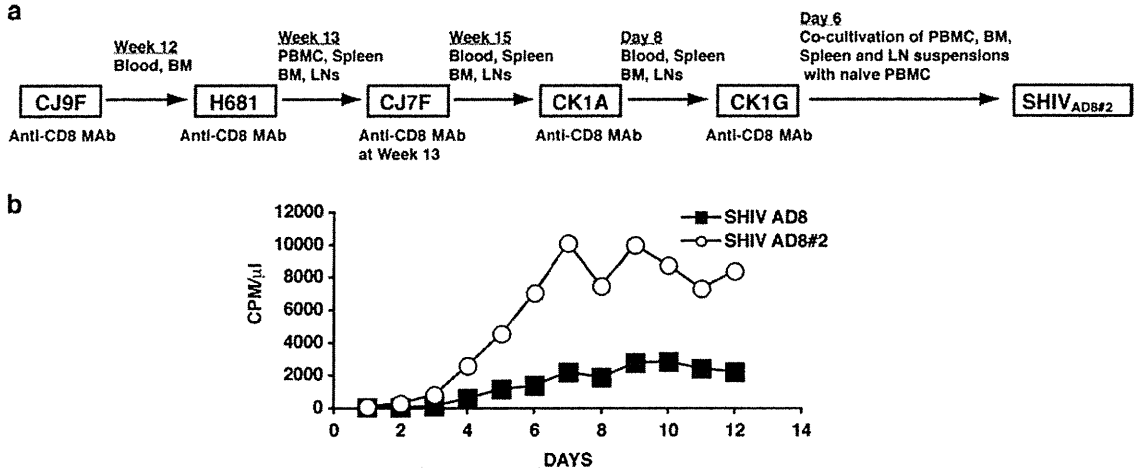

FIG. 2. Serial animal-to-animal passage of $SHIV_{AD8}$. (a) Passage history of $SHIV_{AD8}$ and origin of $SHIV_{AD8\#2}$. (b) Rhesus monkey PBMC were infected with $SHIV_{AD8}$ or the passaged $SHIV_{AD8\#2}$ virus stock, normalized for RT activity. CPM, counts per minute.

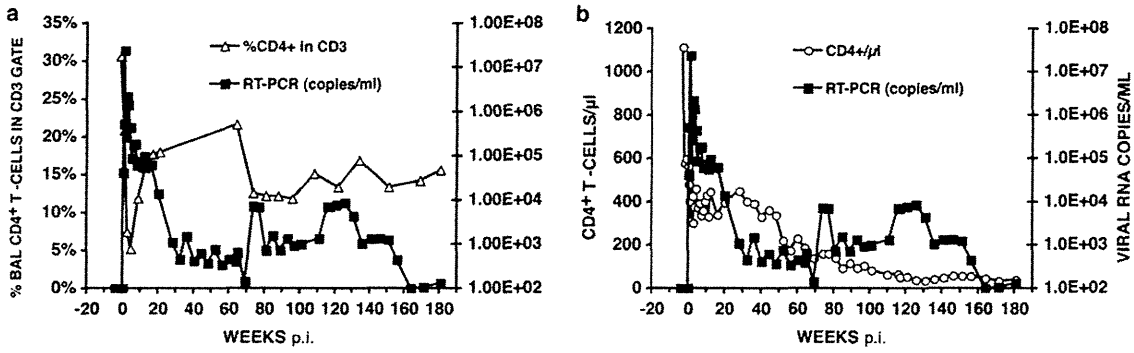

FIG. 3. SHIV$_{AD8\#2}$ induces sustained plasma viremia and loss of CD4 T cells in an inoculated rhesus macaque. Plasma viremia and the percentage of BAL fluid CD4$^+$ T cells (a) or the absolute numbers of circulating CD4$^+$ T cells (b) in rhesus macaque CJ8B inoculated intravenously with SHIV$_{AD8\#2}$ are shown. RT-PCR, reverse transcription-PCR.

14 p.i. CJ7F was euthanized at week 15 p.i., and cell suspensions were prepared as described above and transferred by the i.v., i.p., and BM routes into macaque CK1A, previously treated with anti-CD8 MAb (Fig. 2a). Following the fifth *in vivo* passage, macaque CK1G was euthanized on day 6 p.i., and cell suspensions, prepared at the time of necropsy, were cocultivated with ConA-stimulated PBMC from uninfected rhesus monkeys as described in Materials and Methods; the culture supernatants were monitored for the presence of reverse transcriptase activity, pooled, and designated SHIV$_{AD8\#2}$.

Inoculation of rhesus macaques with SHIV$_{AD8\#2}$ and its immediate derivatives resulted in sustained plasma viremia and loss of CD4$^+$ T lymphocytes. To ascertain whether serial passaging of SHIV$_{AD8}$ *in vivo* had resulted in the acquisition of improved replicative properties, ConA-stimulated rhesus monkey PBMC were infected with SHIV$_{AD8\#2}$ or the starting SHIV$_{AD8}$ virus preparation, both normalized for RT activity. As shown in Fig. 2b, SHIV$_{AD8\#2}$ replicated to much higher levels in cultured macaque PBMC than the original SHIV$_{AD8}$. To determine whether this improved infectivity of SHIV$_{AD8\#2}$ for rhesus PBMC was correlated with augmented replication in an animal not treated with the depleting anti-CD8 MAb, macaque CJ8B was inoculated i.v. with 1.5×10^4 TCID$_{50}$ of SHIV$_{AD8\#2}$. As shown in Fig. 3a, this monkey experienced a marked but transient depletion of memory CD4$^+$ T cells in BAL specimens during the acute infection and maintained detectable levels of plasma viremia. Because animal CJ8B subsequently experienced a decline in the total circulating CD4$^+$ T lymphocyte population from 565 to 175 cells/µl at week 56 p.i. (Fig. 3b), whole blood or virus propagated ex vivo from CJ8B lymph node suspensions (lymph node virus [SHIV$_{AD8LN}$]) was inoculated into four additional macaques (CK15, CJ58, CE8J, and CJ35) (Fig. 4). Four other animals (DB99, DA1Z, A4E008, and DA4W) received blood transfusions, and two (CJ3V and CK5G) were inoculated with PBMC coculture virus (SHIV$_{AD8PBMC}$) derived from monkeys CK15 and CJ58 (Fig. 4). In addition, because it was unknown at the time of its preparation whether SHIV$_{AD8\#2}$ had acquired augmented *in vivo* infectivity properties, SHIV$_{AD8\#2}$ was propagated for an additional 30 days *ex vivo* in macaque PBMC as described in Materials and Methods. Because the resulting derivative, designated SHIV$_{AD8\#2.d30}$, exhibited robust infectivity in both pigtailed and rhesus macaque PBMC (data not shown), it was inoculated intravenously into two rhesus monkeys (CL5A and CL98) (Fig. 4). The inocula used to infect rhesus monkeys with SHIV$_{AD8\#2}$ and its immediate derivatives are listed in Table 1. None of these monkeys received the depleting anti-CD8 MAb.

Ten of the 13 animals infected with SHIV$_{AD8\#2}$ or its immediate derivatives experienced an NP clinical course characterized by set-point virus loads that varied widely (from less than 10^3 to more than 10^5 RNA copies/ml) and a gradual depletion of circulating CD4$^+$ T lymphocytes (Fig. 5a and b). Transient, and in some cases quite significant, losses of memory CD4$^+$ T cells in BAL samples was a common finding during the acute infection (Fig. 5c). The loss of circulating CD4$^+$ T lymphocytes in the 10 SHIV$_{AD8\#2}$-infected NPs affected both memory and naïve subsets (Fig. 6). With one exception (monkey CJ35), these animals sustained depletions of circulating memory CD4$^+$ T cells to the 200-cell/µl level by week 100. NPs also experienced increased memory CD4$^+$ T lymphocyte turnover, as monitored by Ki-67 expression, particularly during the first 10 weeks and the final stages of the infection (see Fig. S1 in the supplemental material). The loss of naïve CD4$^+$ T lymphocytes in NP monkeys was even more profound. By week 80 p.i., this subset had declined to below 100 cells/µl in all of the animals (Fig. 6b). At the time of their euthanasia, five NPs (CJ8B, CE8J, CJ3V, CK15, and CL98) had only 1, 3, 6, 12, and 68 circulating naïve CD4$^+$ T cells/µl, respectively. We previously reported that SIVsmE543-infected

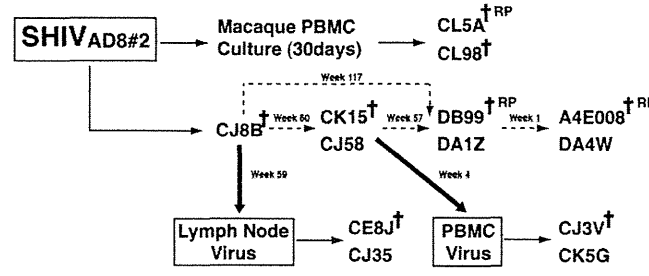

FIG. 4. SHIV$_{AD8\#2}$ and its immediate derivatives cause immunodeficiency in rhesus macaques. The dashed arrows indicate virus transfer by blood transfusion. The thick arrows indicate LN or PBMC specimens used to generate virus stocks by coculturing with PBMC from uninfected donors. †, euthanized animals.

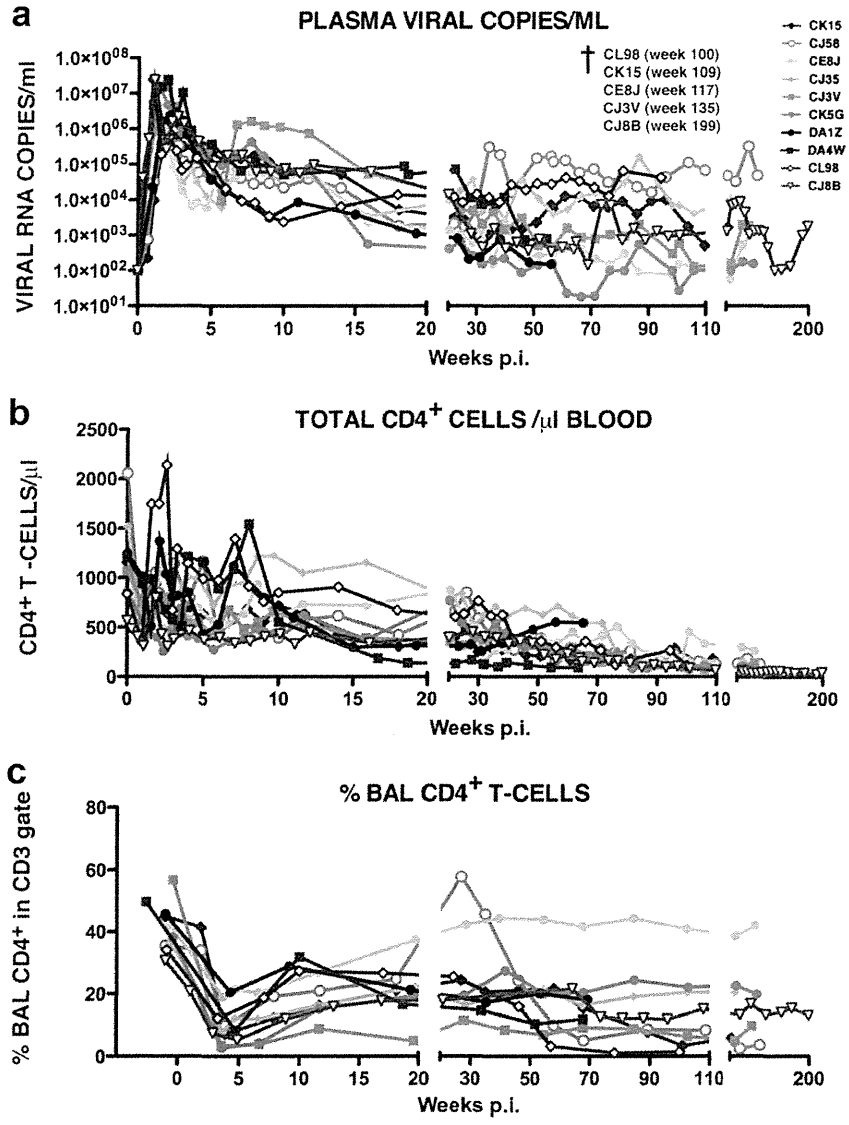

FIG. 5. Total $CD4^+$ T lymphocytes are gradually lost in normal progressors following infection with $SHIV_{AD8\#2}$ and its immediate derivatives. The levels of plasma viremia (a), absolute numbers of peripheral $CD4^+$ T cells (b), and percentages of BAL fluid $CD4^+$ T cells (c) are shown. The five normal progressors that developed AIDS and were euthanized are indicated (†).

NPs had also experienced a marked loss of naïve $CD4^+$ T cells as early as 20 weeks p.i. (35). It was therefore not unexpected that NP $SHIV_{AD8}$-infected monkeys might also sustain a depletion of their naïve $CD4^+$ T cell subset.

Three of the 13 macaques inoculated with $SHIV_{AD8\#2}$ and its immediate derivatives became RPs, requiring euthanasia between weeks 19 and 23 p.i. because of anorexia, intractable diarrhea, and marked weight loss (Fig. 7). Virus set points in the RPs exceeded 10^7 RNA copies/ml, memory $CD4^+$ T cells in BAL specimens rapidly and irreversibly declined, and at the time of death, all of the animals had sustained marked losses of circulating $CD4^+$ T cells.

Immune responses to $SHIV_{AD8}$. In the context of its use as a challenge virus in vaccine experiments, it was important to show that $SHIV_{AD8}$ elicited both cellular and humoral immune responses during infections of rhesus monkeys. Therefore, anti-$SHIV_{AD8}$ Gag-specific $CD8^+$ T lymphocyte responses were measured by flow cytometry for 6 of the 10 NPs by intracellular staining of cells expressing TNF-α and/or IFN-γ following stimulation with a 15-mer peptide pool spanning SIV_{mac239} Gag. The levels of virus-specific $CD8^+$ T cells in this group of rhesus monkeys ranged from 0.33 to 1.68% during the second year of their infection (see the table in the supplemental material). A similar analysis of Gag-specific responses in memory $CD4^+$ T cells at these times in the same animals indicated that 0.90 to 2.90% expressed TNF-α and/or IFN-γ (see the table in the supplemental material).

NAbs were detected in several of the NPs during the course of their infections (Fig. 8). The seven macaques evaluated had been inoculated with $SHIV_{AD8\#2}$ or two immediate derivatives ($SHIV_{AD8\#2LN}$ and $SHIV_{AD8\#2PBMC}$). Plasma neutralizing activity directed against the same virus used for animal challenge was evaluated in monkeys CJ8B, CE8J, CJ35, CJ3V, and

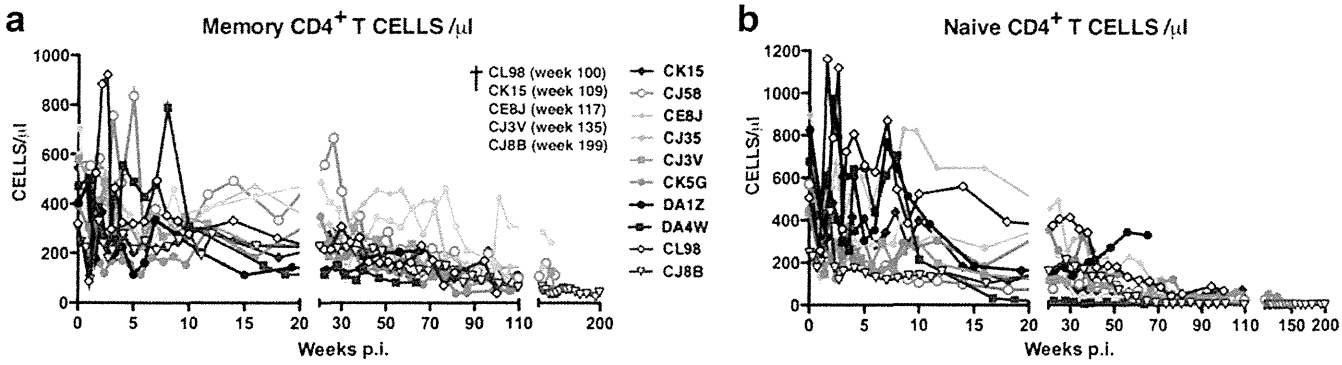

FIG. 6. Marked depletion of naïve and memory CD4$^+$ T lymphocytes characterizes long-term SHIV$_{AD8}$ infection in NP rhesus monkeys. Absolute numbers of memory CD4$^+$ T cells (a) and naive CD4$^+$ T cells (b) in 10 normal-progressor macaques during 200 weeks of SHIV$_{AD8}$ infection are shown. †, euthanized animals.

CK5G. The neutralization sensitivity of autologous virus (SHIV$_{AD8\#2PBMC}$) was monitored using plasma collected from PBMC of macaques CK15 and CJ58 (Fig. 4). The time of appearance of neutralization activity varied widely (week 20 to week 78 p.i.) and was generally correlated with levels of set-point viremia. In the three macaques producing the highest levels of anti-SHIV$_{AD8}$ NAbs, the actual 50% inhibitory concentration (IC_{50}) neutralization titers determined by limiting plasma dilution were 1:159 (CJ8B at week 89), 1:102 (CJ58 at week 30), and 1:143 (CE8J at week 52).

Coreceptor usage by SHIV$_{AD8}$ lineage viruses. The *env* gene of SHIV$_{AD8}$ was derived from the prototypical macrophage-tropic HIV-1$_{Ada}$, previously shown to use CCR5 for cell entry (53). When tested in a TZM-bl entry assay with inhibitors that specifically target CXCR4 or CCR5, the original SHIV$_{AD8}$, SHIV$_{AD8\#2}$ (data not shown), and SHIV$_{AD8\#2LN}$ exclusively utilized CCR5 (see Fig. S2 in the supplemental material). The marked depletion of circulating naïve CD4$^+$ T cells in all SHIV$_{AD8}$ NPs (Fig. 6b) raised the possibility that a coreceptor switch had occurred, enabling these viruses to enter and eliminate naïve CD4$^+$ T cells, which express high levels of surface CXCR4, but not CCR5. Accordingly, virus was recovered from three NPs (CK15, CE8J, and CL98) immediately prior to euthanasia. When tested for coreceptor usage, the viruses isolated from all three NPs remained R5 tropic (see Fig. S2 in the supplemental material), indicating that the loss of naïve CD4$^+$ T cells was not due to direct virus-induced cell killing.

As noted earlier, three monkeys infected with SHIV$_{AD8\#2}$ derivatives exhibited an RP phenotype. By week 10 p.i., these macaques (DB99, A4E008, and CL5A) had experienced massive loss of memory CD4$^+$ T cells in samples collected by BAL (Fig. 7c) but had little change in the number of circulating naive CD4$^+$ T lymphocytes (data not shown). However, by week 19 p.i., the levels of total CD4$^+$ T cells in the blood had declined significantly in all three RPs (Fig. 7b), raising again the possibility that coreceptor usage might have changed. To assess a possible coreceptor switch, virus was collected from RP monkeys DB99 and A4E008 at the time of euthanasia and evaluated in the TZM-bl assay with specific CXCR4 and CCR5 inhibitors. As shown in Fig. 9a, blocking the entry of SHIV$_{AD8\text{-}DB99}$ required both inhibitors, whereas SHIV$_{AD8\text{-}A4E008}$ was inhibited only by the CCR5 inhibitor. This result indicates that SHIV$_{AD8\text{-}DB99}$ had acquired the capacity to use CXCR4 during its infection of macaque DB99 and that SHIV$_{AD8\text{-}A4E008}$ had remained R5 tropic.

Reverse transcription-PCR cloning and sequencing of *env* genes amplified from the plasma of macaque DB99 at the time of its euthanasia revealed that 28 of 29 recovered clones contained a 3-aa insertion (RIG) located 2 residues upstream of the GPGR sequence in the crown of the gp120 V3 region (Fig. 9b). A similar analysis of the *env* gene from virus circulating in monkey A4E008 revealed a different 3-aa insertion (HIG) at the same location in its V3 loop. The V3 loop sequences amplified from the plasma of both animals at week 2 p.i. did not contain any insertion. The gp120 region amplified from the third RP (macaque CL5A) at the time of euthanasia contained no insertion (Fig. 9b).

One of the 28 viral-DNA clones amplified from macaque DB99 plasma at the time of euthanasia containing the RIG insertion in V3 and the single clone simultaneously obtained from this animal lacking the V3 insertion were used to prepare pseudotyped virus for testing in the entry assay, as described in Materials and Methods. As shown in Fig. 9c, the V3 RIG insertion conferred usage of both CCR5 and CXCR4 coreceptors on SHIV$_{psAD8(RIG+)}$ compared to the exclusive utilization of CCR5 by SHIV$_{psAD8(RIG-)}$, which lacks the gp120 V3 insertion.

SHIV$_{AD8}$-infected macaques developed immunodeficiency. The clinical statuses and disease outcomes of all 13 animals inoculated with SHIV$_{AD8\#2}$ and its immediate derivatives during a 2- to 3-year observation period are presented in Table 2. As noted above, 10 of these 13 macaques were NPs and experienced gradual and irreversible depletions of both memory and naïve CD4$^+$ T lymphocyte subsets (Fig. 6). Five of these animals were euthanized with symptoms of AIDS, and 3 additional NPs currently have CD4$^+$ T cell counts ranging from 92 to 154 cells/μl plasma (Table 2). Histopathological studies performed on specimens collected at the time of necropsy revealed the presence of *Pneumocystis carinii*, *Mycobacterium avium*, and *Campylobacter coli* infections in individual macaques (see Fig. S3 in the supplemental material). In addition, 3 of the 13 R5-SHIV-infected monkeys experienced an RP syndrome characterized by sustained plasma viremia of

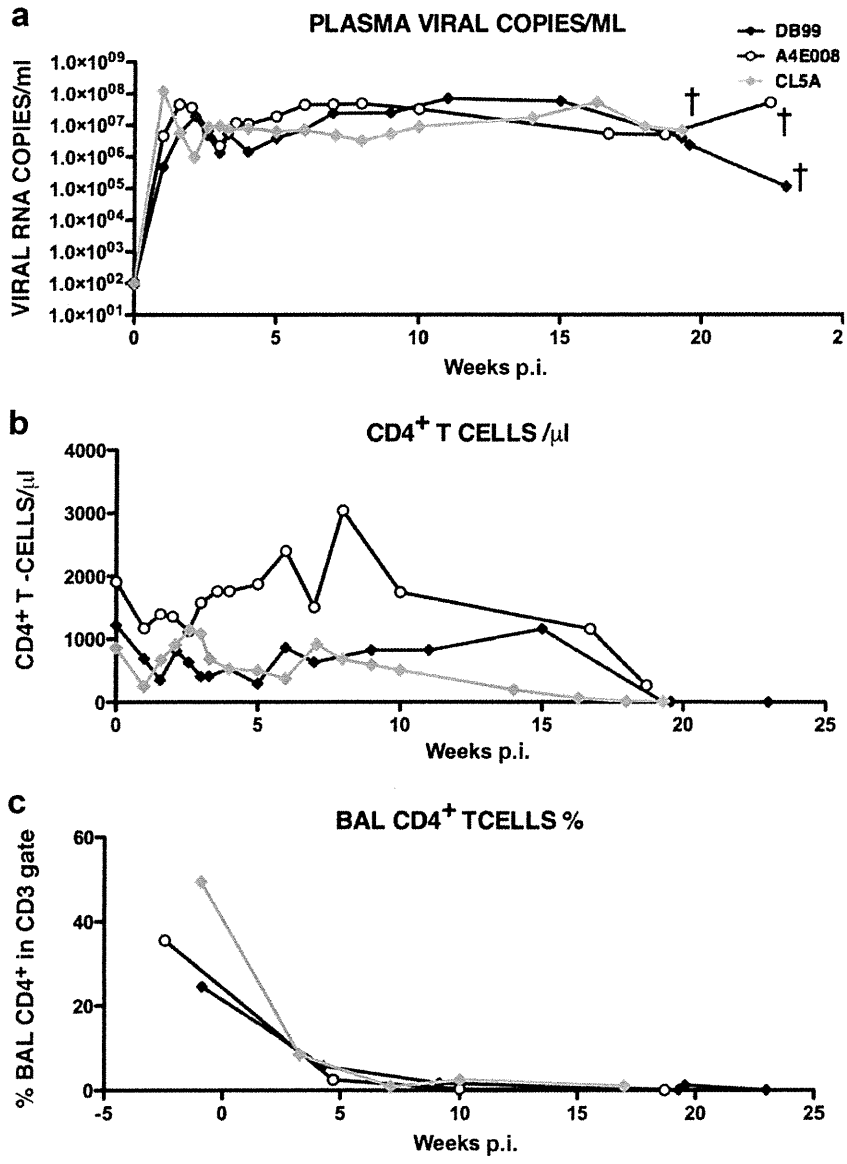

FIG. 7. Patterns of virus replication and CD4+T cell dynamics in $SHIV_{AD8}$ rapid progressors. The levels of plasma viremia (a), absolute numbers of peripheral $CD4^+$ T cells (b), and percentages of BAL fluid $CD4^+$ T cells (c) are shown. †, euthanized animals.

$>1 \times 10^7$ RNA copies/ml; rapid and irreversible loss of memory $CD4^+$ T cells in the blood and at an effector site (BAL); and intractable diarrhea, anorexia, and weight loss requiring euthanasia between weeks 19 and 23 p.i.

DISCUSSION

The results presented clearly show that the generation of a pathogenic R5-SHIV was not a trivial undertaking. Animal-to-animal passaging eventually gave rise to $SHIV_{AD8\#2}$, possessing greatly augmented infectivity for rhesus PBMC compared to the starting $SHIV_{AD8}$ construct. Although it was not appreciated at the time, $SHIV_{AD8\#2}$ had also acquired improved *in vivo* properties, as evidenced by its and its immediate derivatives' capacity to cause fatal immunodeficiency in 8 of 13 inoculated rhesus monkeys (Fig. 4 and Table 2). The most consistent and distinguishing property of the passaged $SHIV_{AD8}$ family of viruses during infections of rhesus macaques was the slow and unremitting loss of both memory and naïve $CD4^+$ T cells (Fig. 6), a pattern of depletion observed in all 10 NPs. Surprisingly, and in contrast to both SIVmac and SIVsmE lineages, the pace of $CD4^+$ T lymphocyte decline was not correlated with plasma virus loads. Although the geometric mean plasma viral-RNA level at week 50 in the $SHIV_{AD8}$-infected monkey cohort was 1.7×10^3 RNA copies/ml, the set-point virus loads varied widely in the 10 infected animals

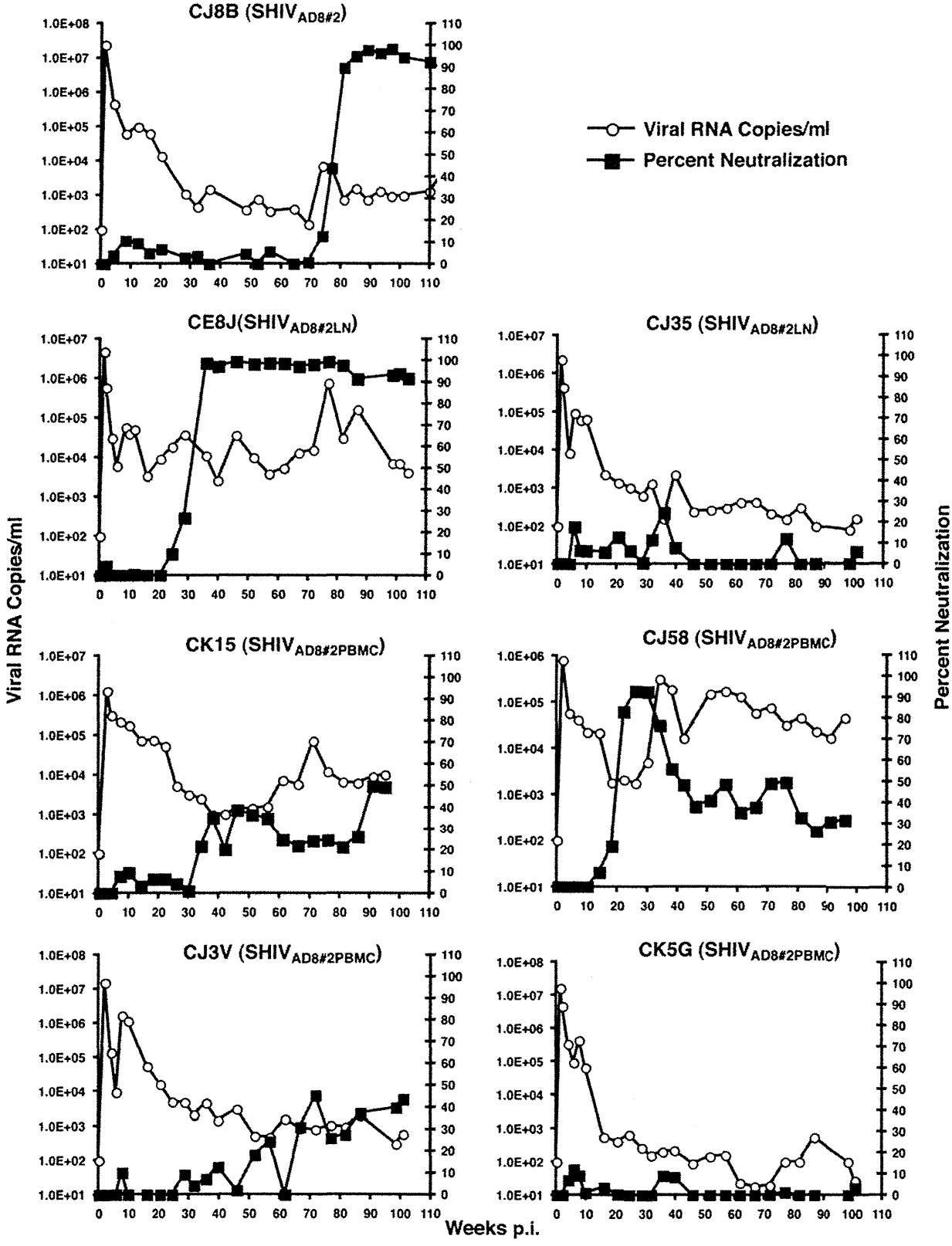

FIG. 8. Neutralizing-antibody activities detected in normal-progressor macaques following infection with SHIV$_{AD8\#2}$ or its immediate derivatives. Plasma samples (1:20 dilution) from the indicated SHIV$_{AD8}$-infected macaques were incubated in quadruplicate for 1 h at 37°C with the virus isolates shown in parentheses and then used as an inoculum to infect TZM-bl cells. The luciferase activity present in cell lysates at 28 h p.i. was measured, and the average percent neutralization activity in plasma at each time point was determined. Prechallenge plasma samples served as negative controls and baselines for zero neutralizing-antibody activity.